Fragment Distributions of Transfer- and Fusion-Induced Fission in Inverse Kinematics. The Impact of the Excitation Energy.

D. Ramos[1,2], M. Caamaño[1], F. Farget[3], C. Rodríguez-Tajes[3], L. Audouin[2], J. Benlliure[1], E. Casarejos[4], E. Clement[3], D. Cortina[1], O. Delaune[3], X. Derkx[5,*], A. Dijon[3], D. Doré[6], B. Fernández-Domínguez[1], G. de France[3], A. Heinz[7], B. Jacquot[3], A. Navin[3], C. Paradela[1], M. Rejmund[3], T. Roger[3], M.-D. Salsac[6], C. Schmitt[3]

(1) Dpto. Física de Partículas, USC, Santiago de Compostela, Spain. (2) IPN Orsay, Université de Paris-Sud XI - CNRS/IN2P3, Orsay, France. (3) GANIL, CEA/DMS - CNRS/IN2P3, Caen, France. (4) CIMA, Escuela Técnica Superior de Ingenieros Industriales, UVigo, Vigo, Spain. (5) LPC Caen, Université de Caen Basse-Normandie – ENSICAEN - CNRS/IN2P3, Caen, France. (6) CEA Saclay, DSM/IRFU/SPhN, Saclay, France. (7) Chalmes University of Technology, Göteborg, Sweden.

FIESTA 2017, SANTA FE 19/09/2017

Direct kinematics

- Fragments with low energy
- Mass distribution measurements

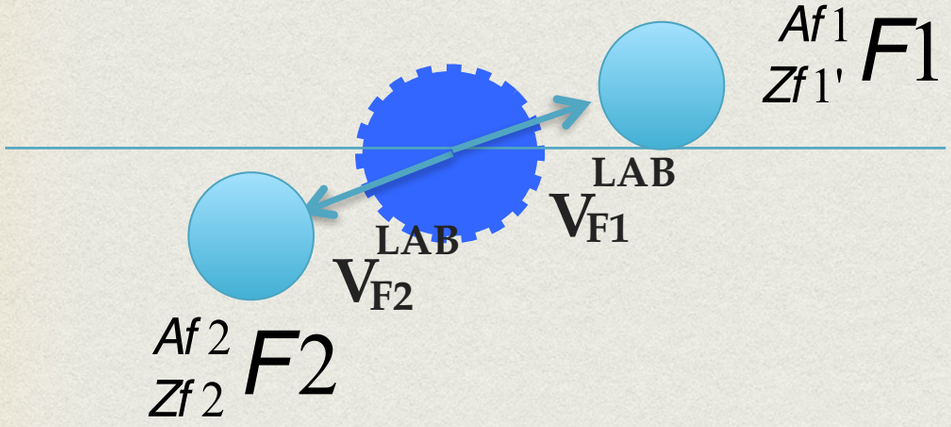

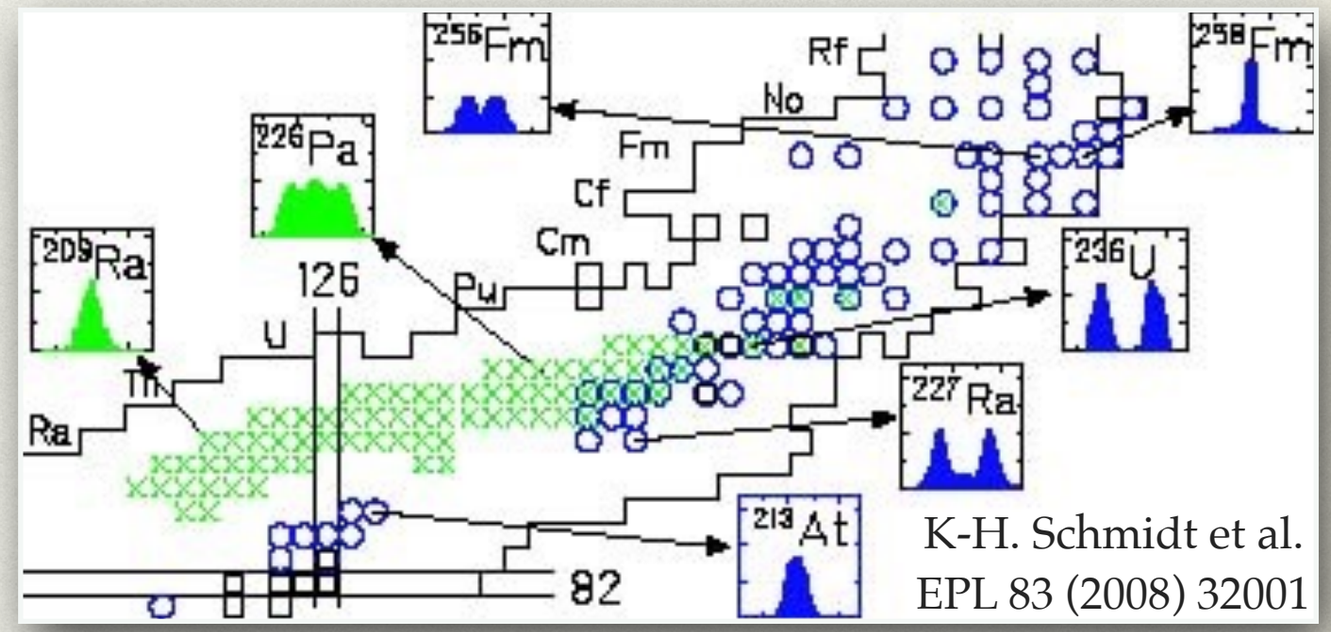

K-H. Schmidt et al.
EPL 83 (2008) 32001

Inverse kinematics

- Fragments with high energy
- Direct Z distribution measurements

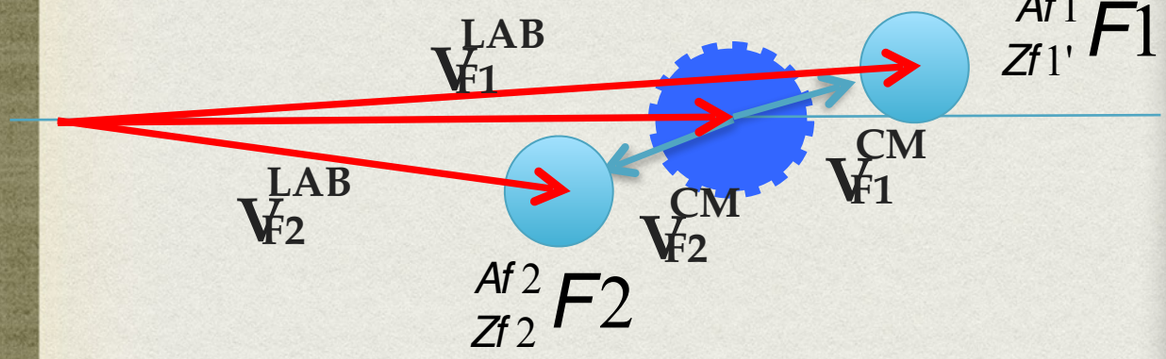

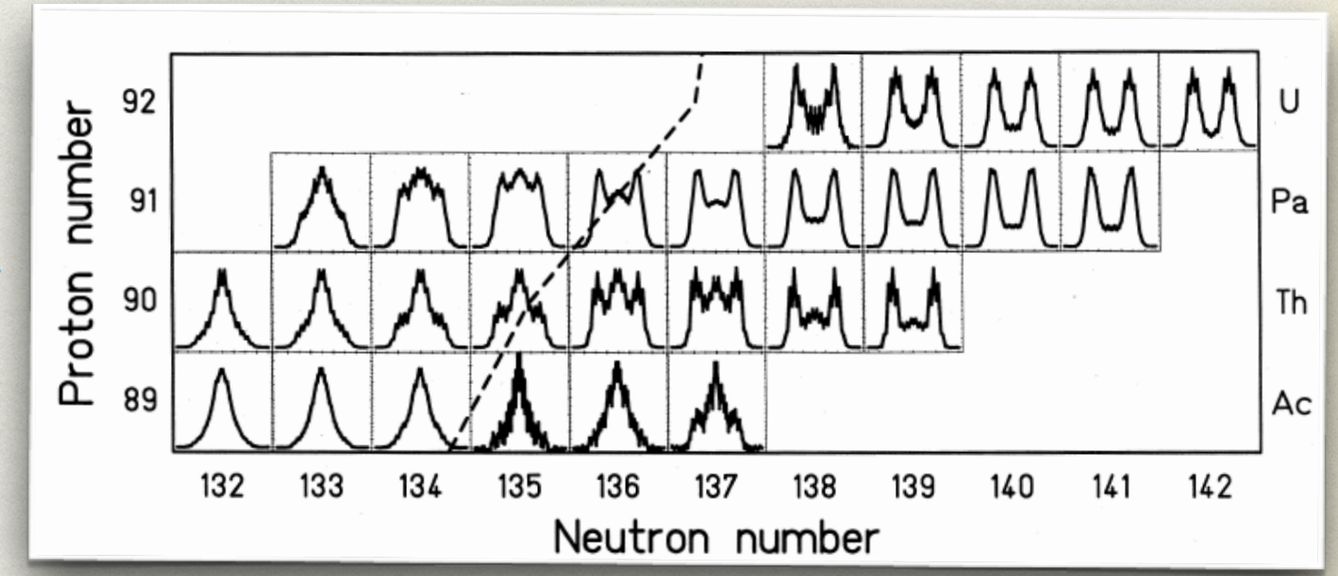

K-H. Schmidt et al. NPA 665 (2000) 221

INVERSE KINEMATICS + MAGNETIC SPECTROMETER → FULL ISOTOPIC FRAGMENT DISTRIBUTION

$^{238}U + ^{12}C$ @ 6.14 AMeV

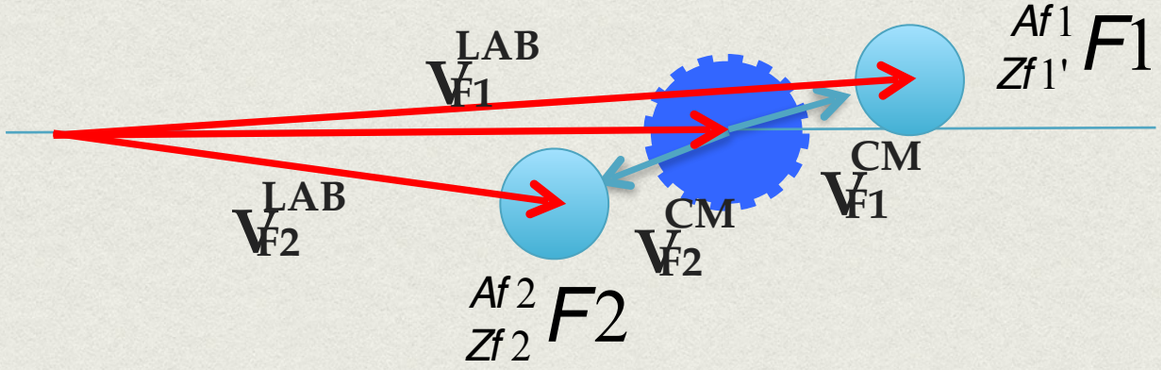

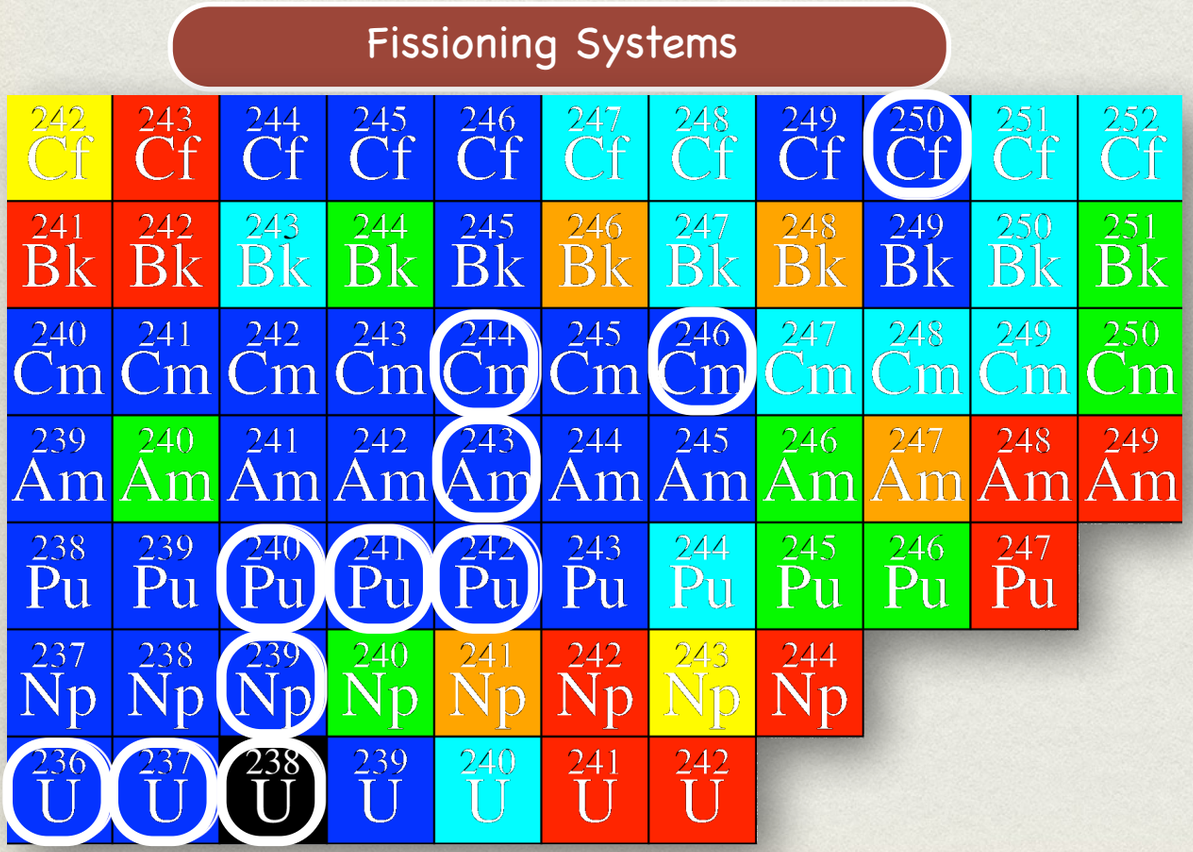

Transfer-Fission:

10 n-rich actinides produced with a distribution of E_X below 30 MeV

Fusion-Fission:

production of ^{250}Cf with $E_X = 46$ MeV
10 times more likely than any transfer channel

EXPERIMENTAL SETUP

-Fissioning system identification
-Exctation energy reconstruction

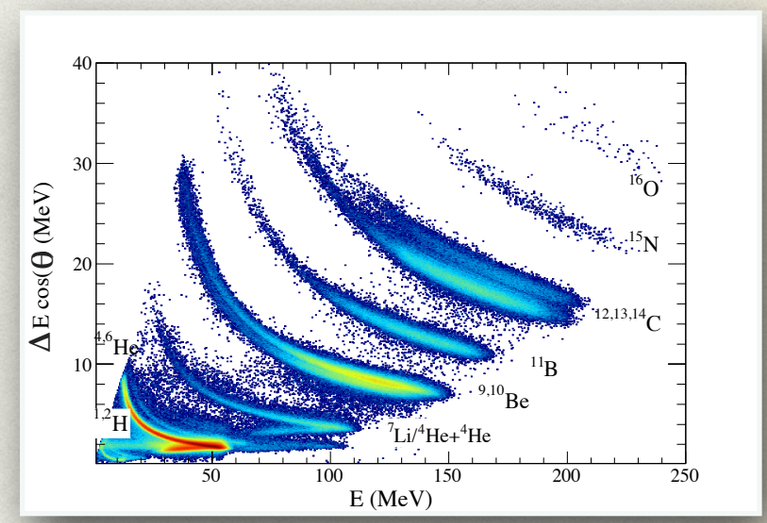

FOCAL PLANE
DETECTION SETUP

dipole

quadrupoles

VAMOS

-Fission fragment identification
-Fission kinematics reconstruction

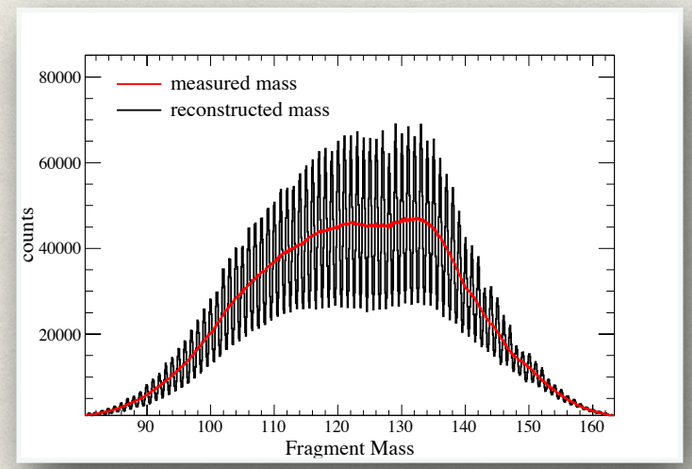

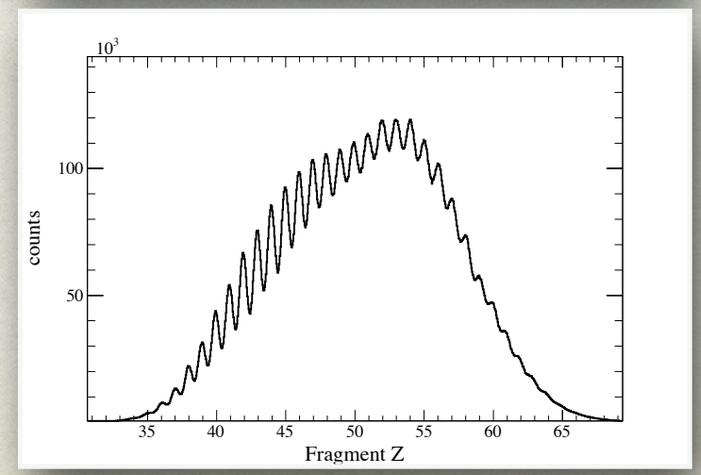

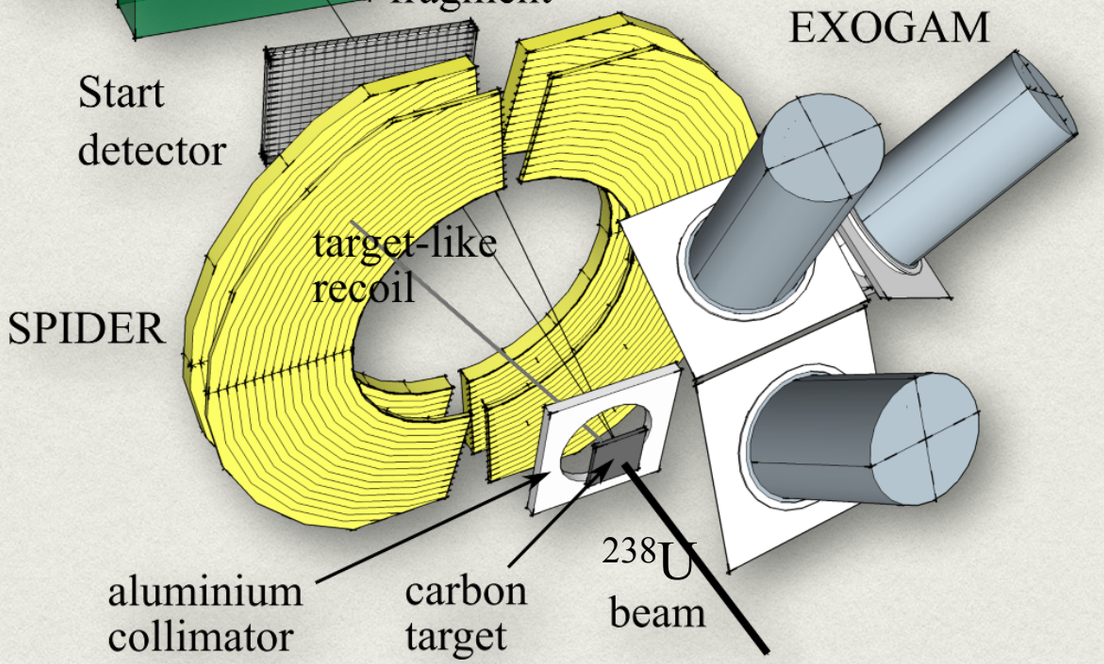

MORE DETAILS IN POSTER

ISOTOPIC FISSION YIELDS

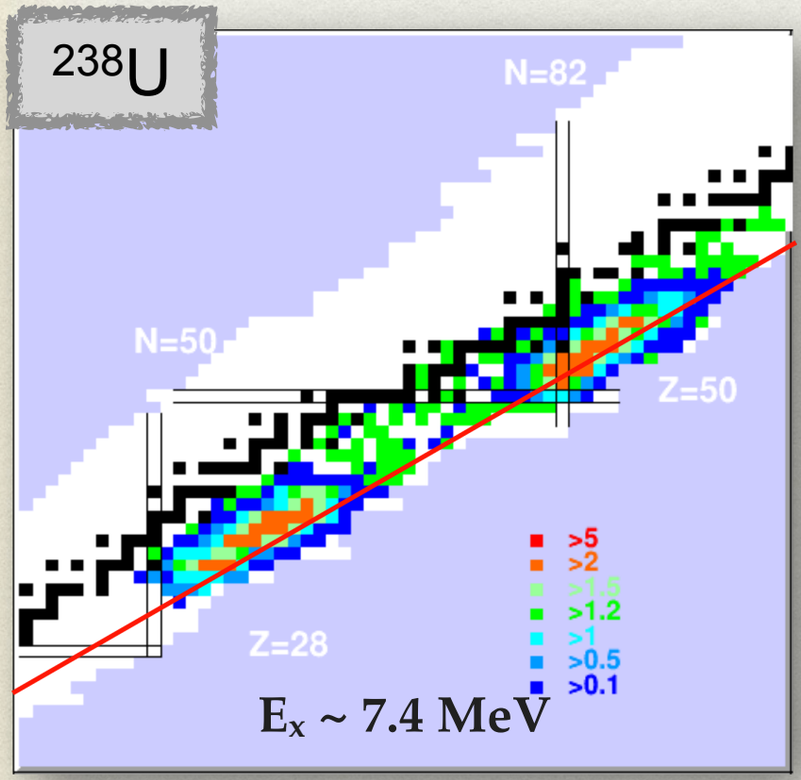

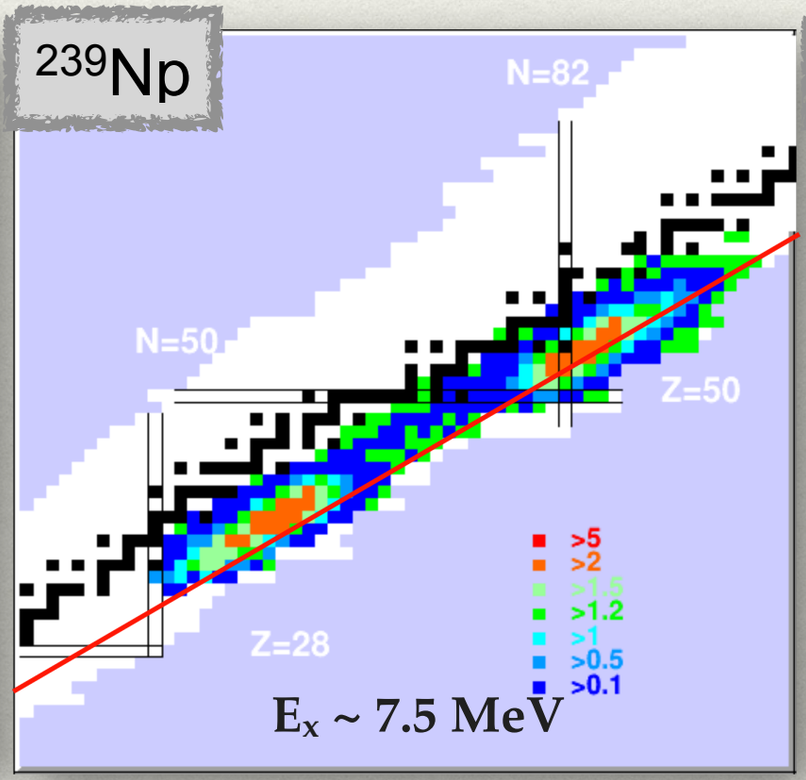

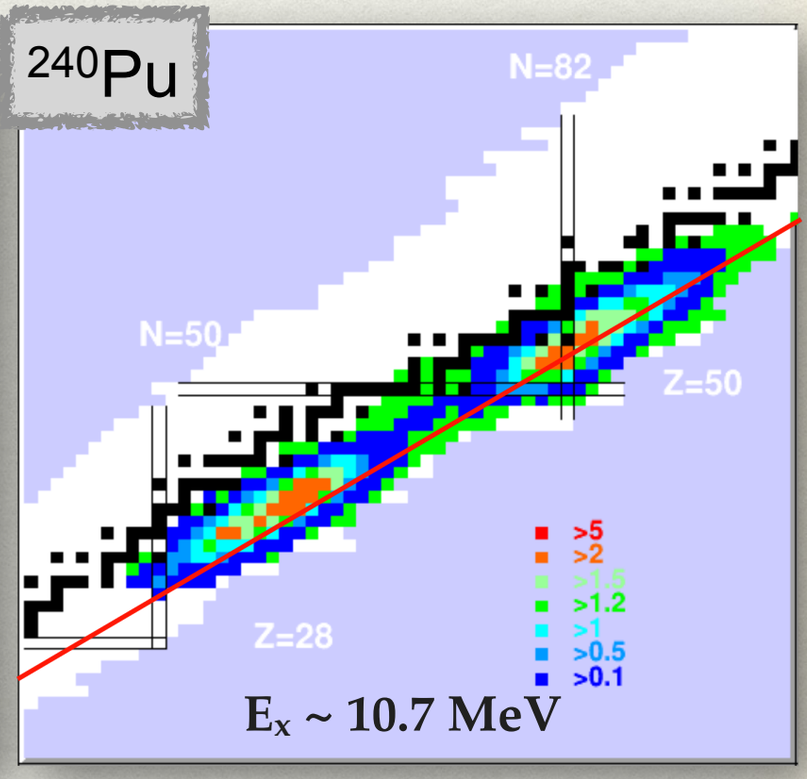

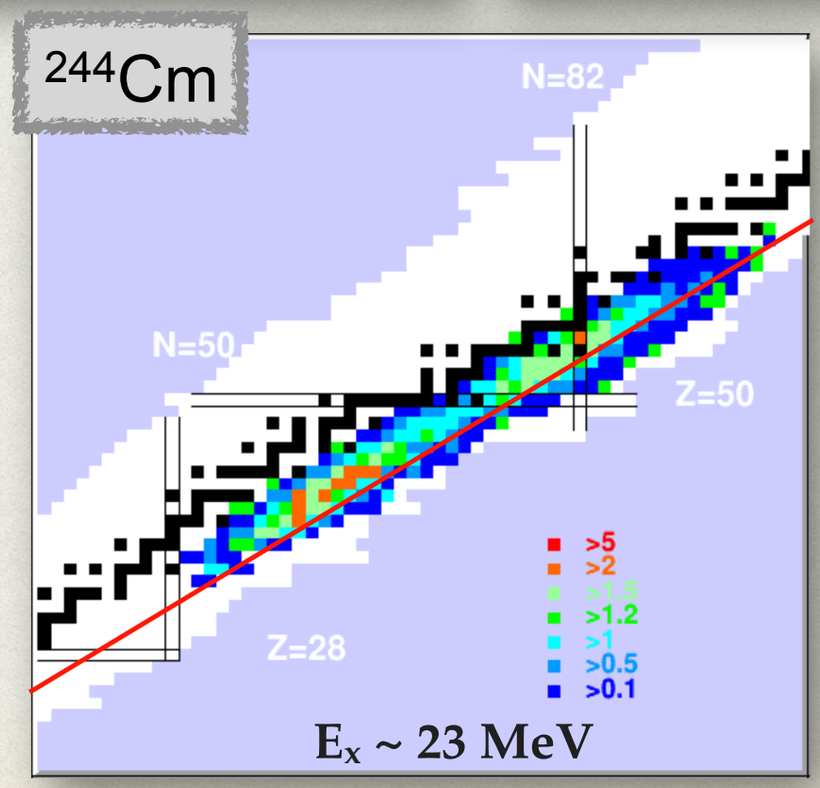

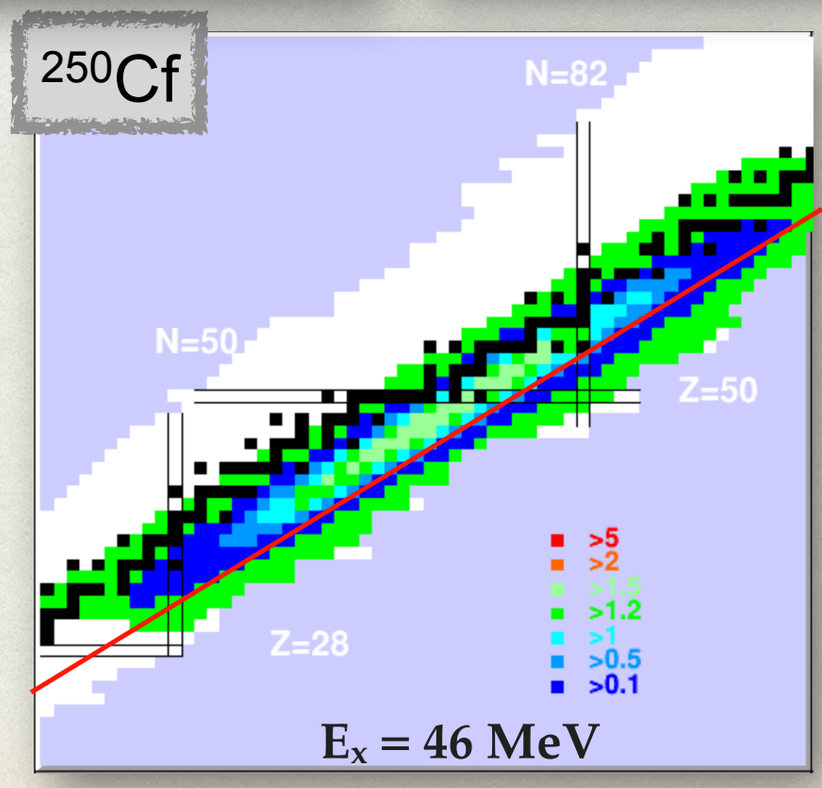

ELEMENTAL FISSION YIELDS

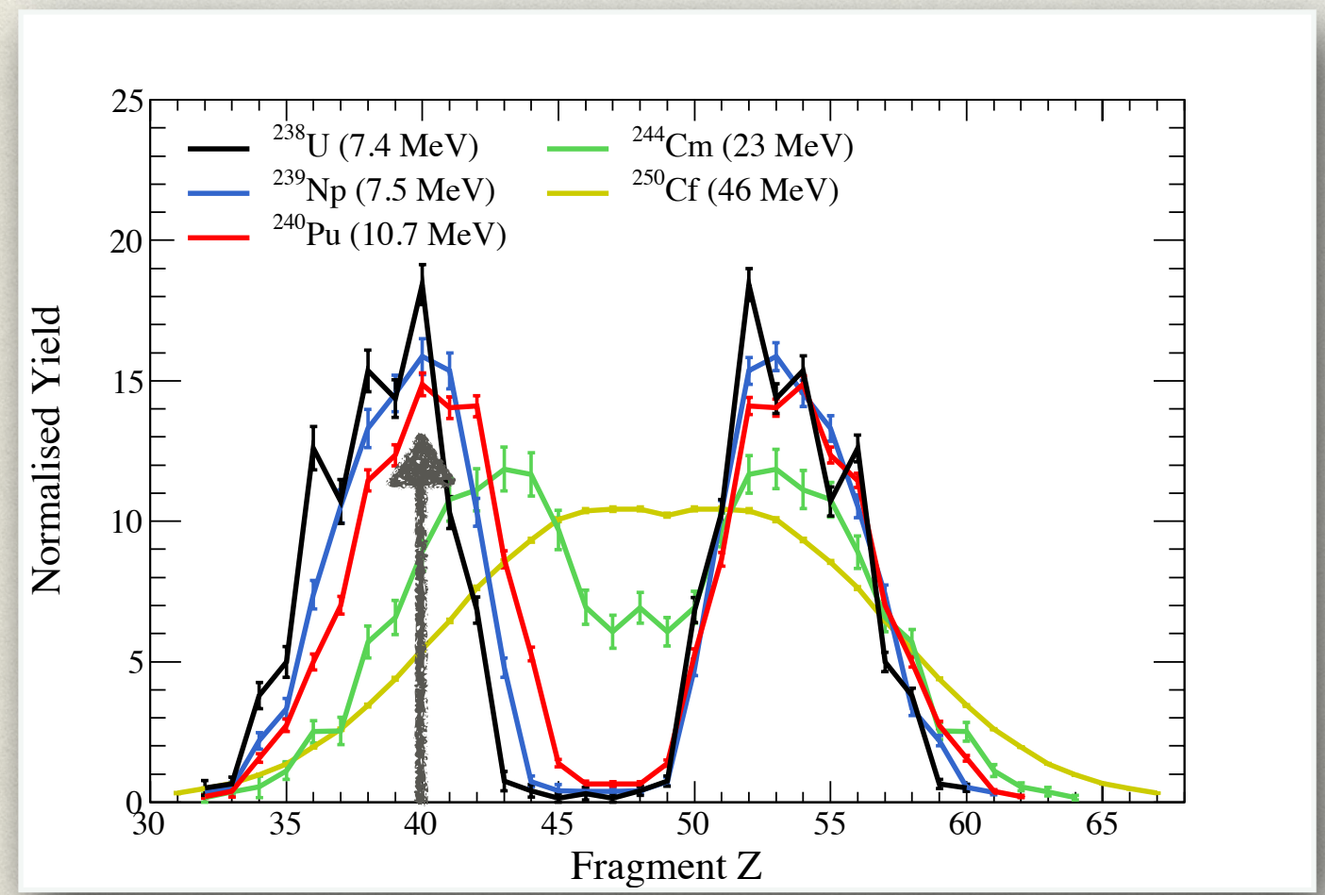

- Stabilization of the heavy fragment
- Light fragment shifted with a constant maximum **Z=40** at low E_x
- Strong even-odd staggering at low E_x in even-Z systems

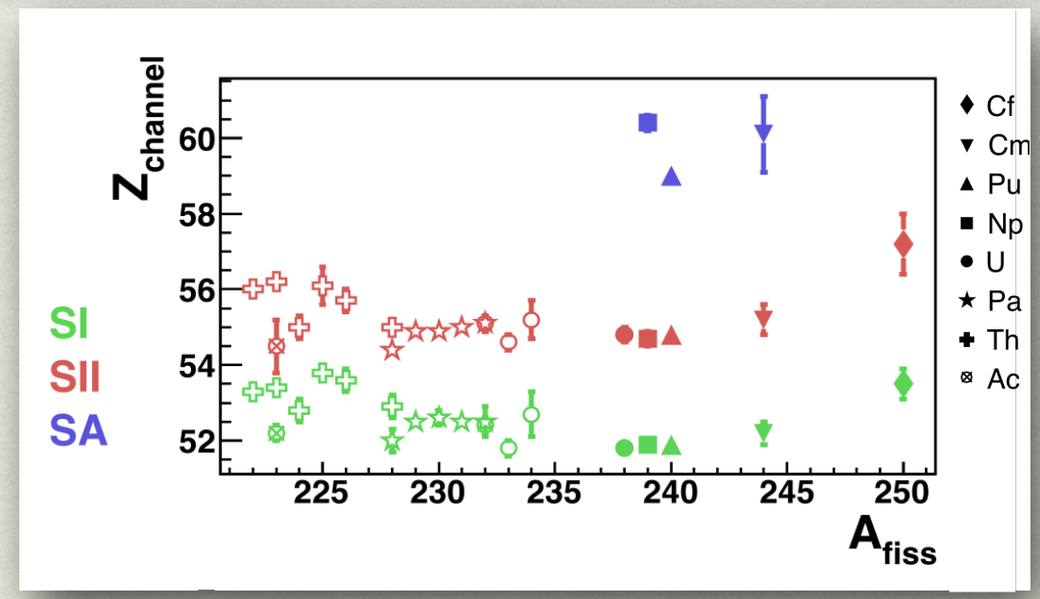

C. Böckstiegel et al. NPA 802(2008)12

- Asymmetric Fission Modes positions:
  (U. Brosa et al. Phys. Reports 197(1990)167)

Standard I : Spherical heavy fragment, compact scission configuration **Z ~52**

Standard II : Deformed heavy fragment **Z ~55**

Z EVEN-ODD STAGGERING

$$\delta\left(Z_i + \frac{3}{2}\right) = \frac{(-1)^{Z_i}}{8} \cdot \left[\ln Y(Z_{i+3}) - \ln Y(Z_i) - 3\left(\ln Y(Z_{i+2}) - \ln Y(Z_{i+1})\right)\right]$$

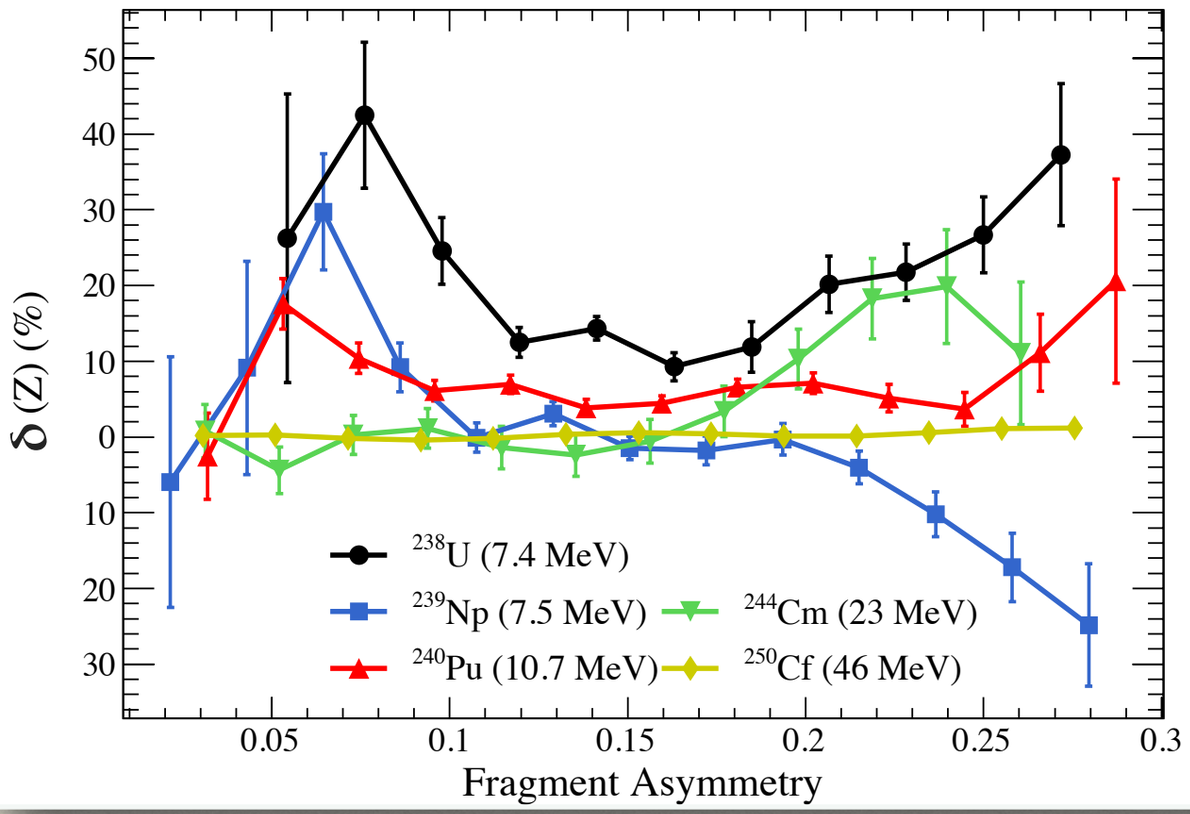

- The even-odd effect increases with the fragment asymmetry with a local maximum around Z~50
- Systems at higher E_x show lower even-odd effect
- Odd-Z nuclei ^{239}Np show oposite behavior

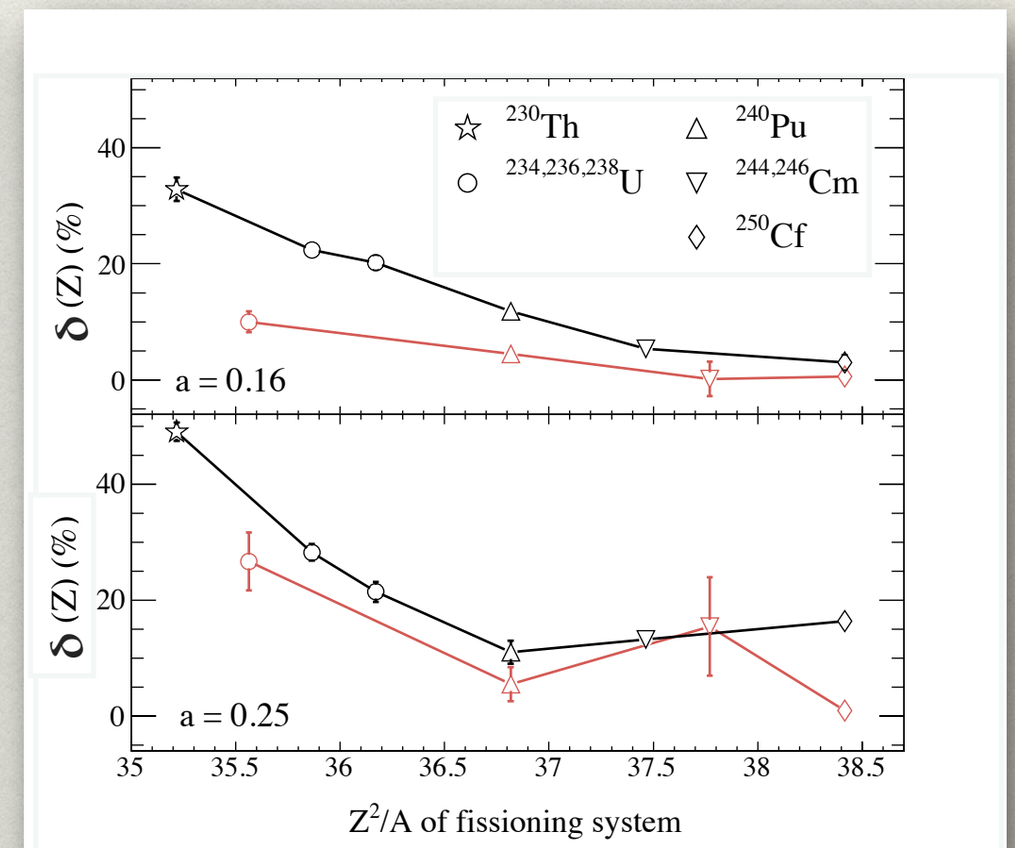

Even-Z nuclei (red) compared with thermal-neutron induced fission (black) at different asymmetries

- **For central asymmetry, the impact of Z^2/A dominates over E_x difference**

NEUNTRON DISTRIBUTIONS AND NEUTRON EXCESS

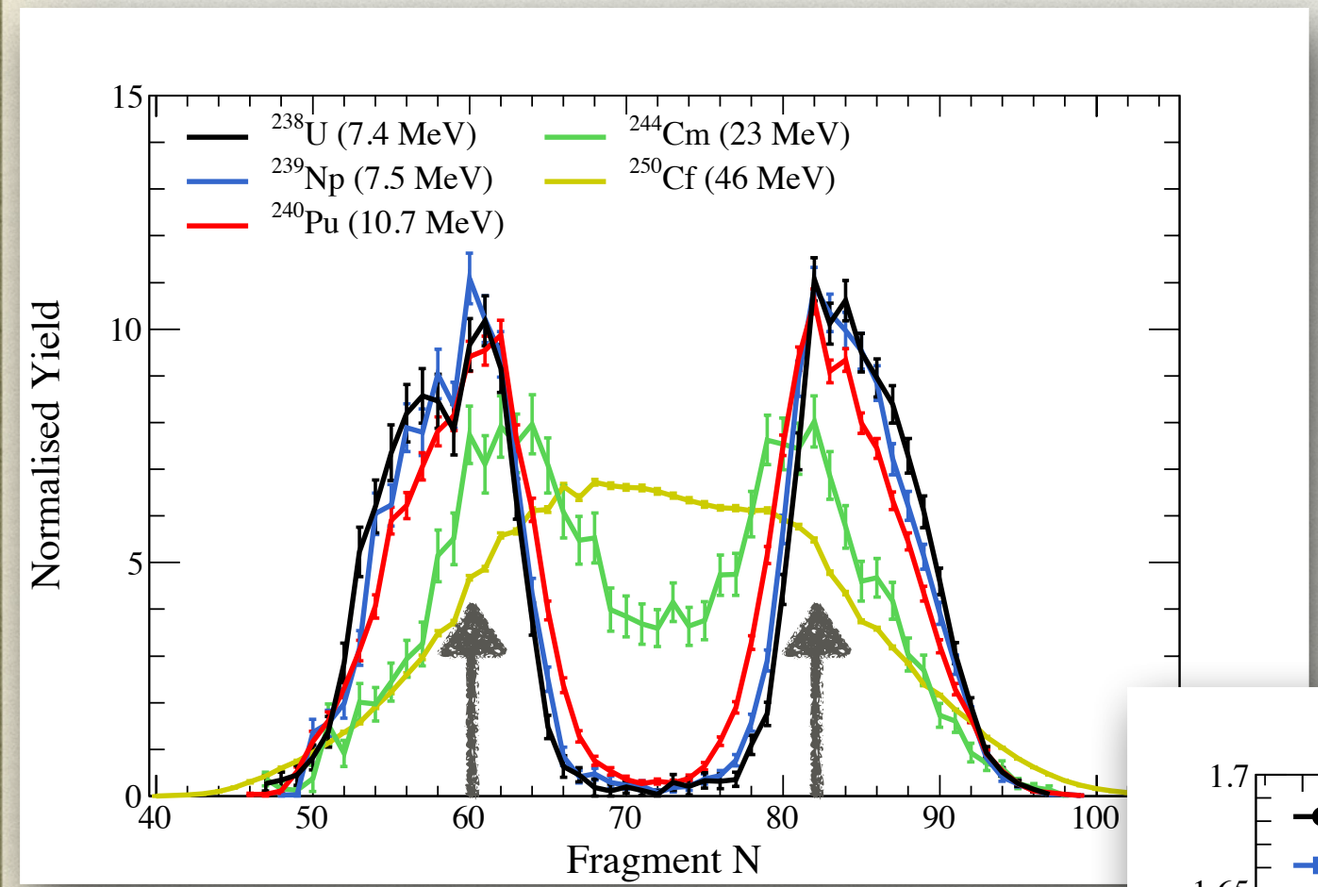

- **Post neutron evaporation**
- Maximum in the heavy fragment at **N=82**
- Unexpected maximum in the light fragment **N~60**
- The no-flat plateau of ^{250}Cf reflects the effect of the increasing neutron evaporation

- **Charge polarization** with the heavy fragment more n-rich than the light fragment
- High <N>/Z at Z~50 at low E_x, decreasing in systems at higher E_x
- Tendency to the double magic nucleus ^{132}Sn
- Local maximum at Z~40

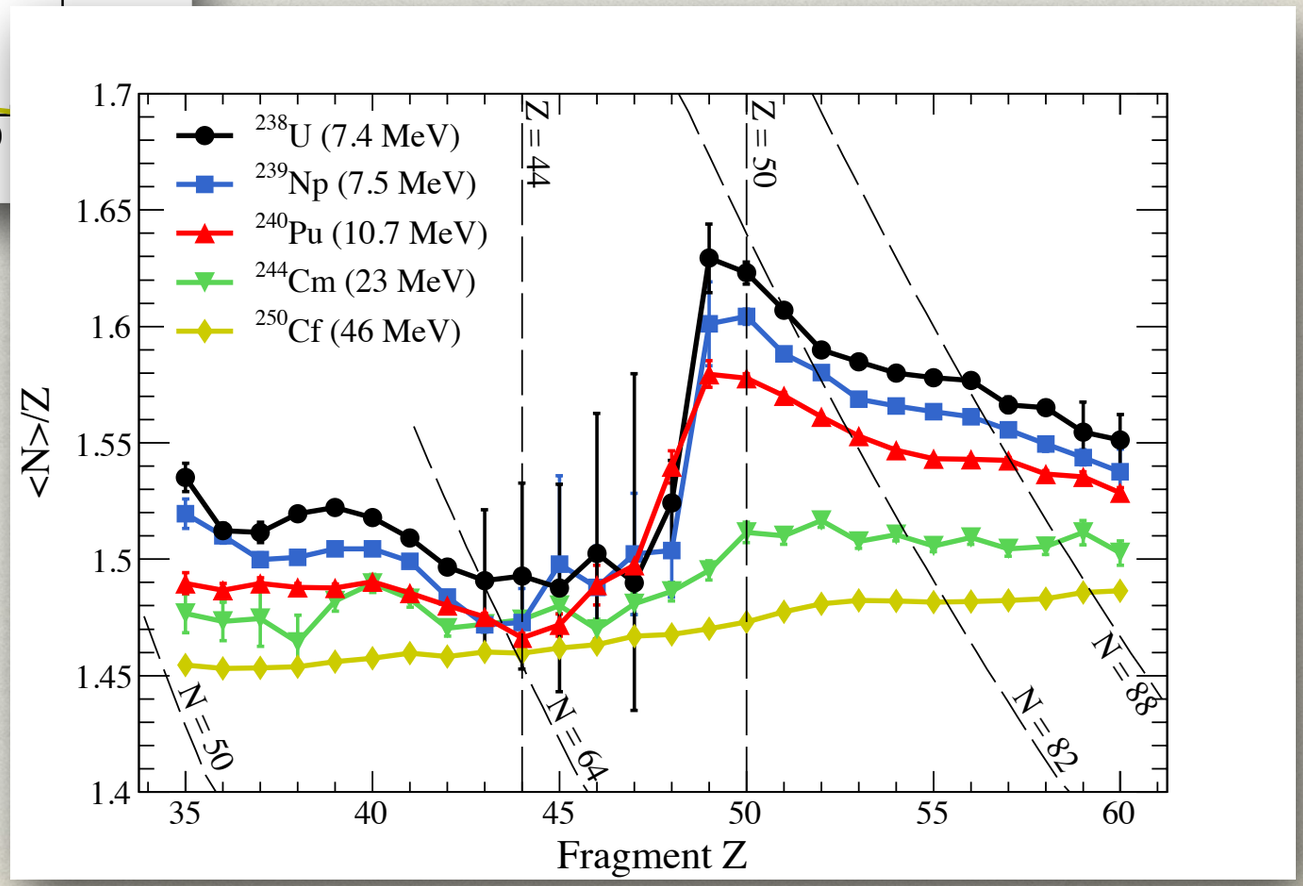

ISOTOPIC DISTRIBUTION IN Z=50

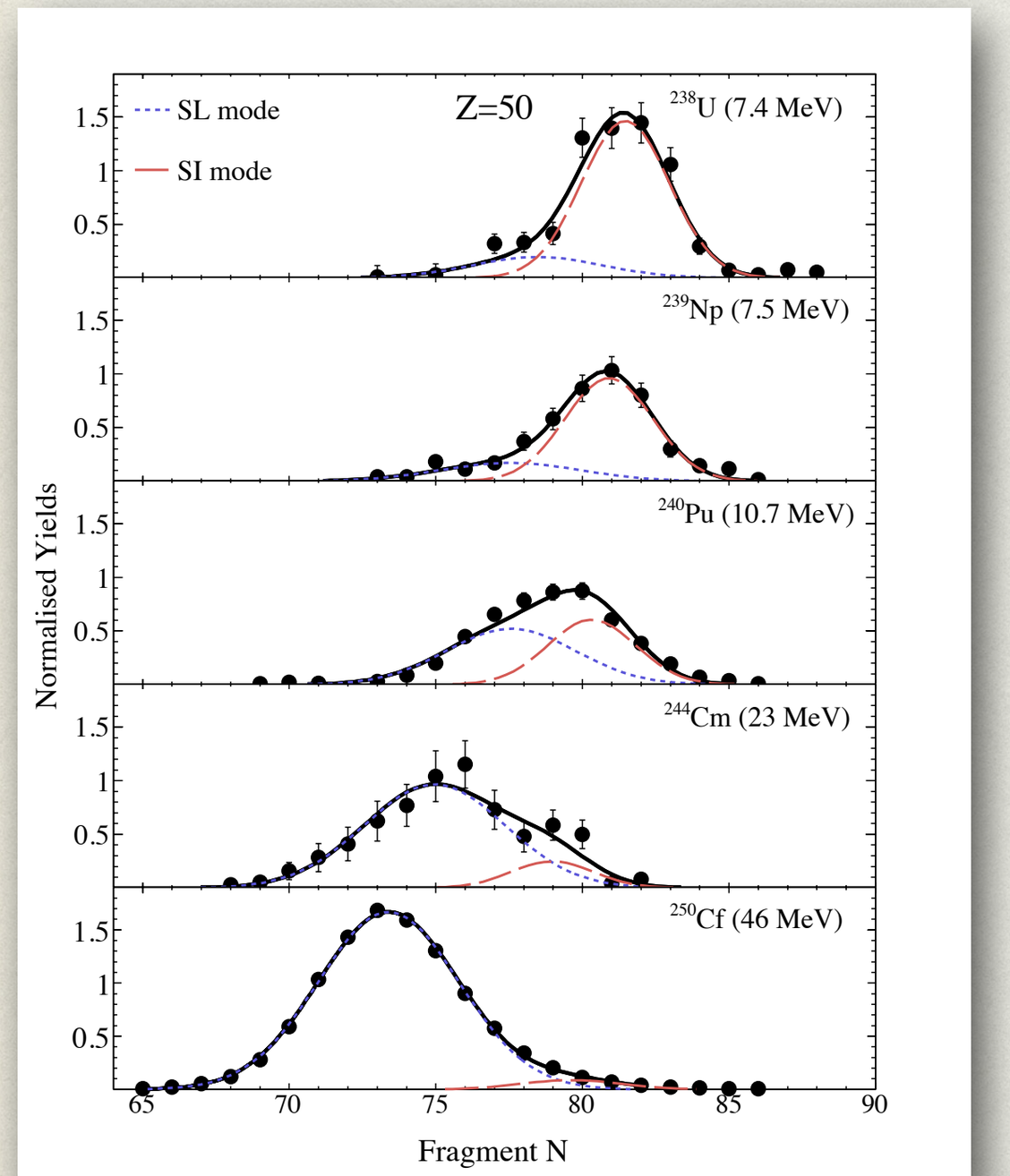

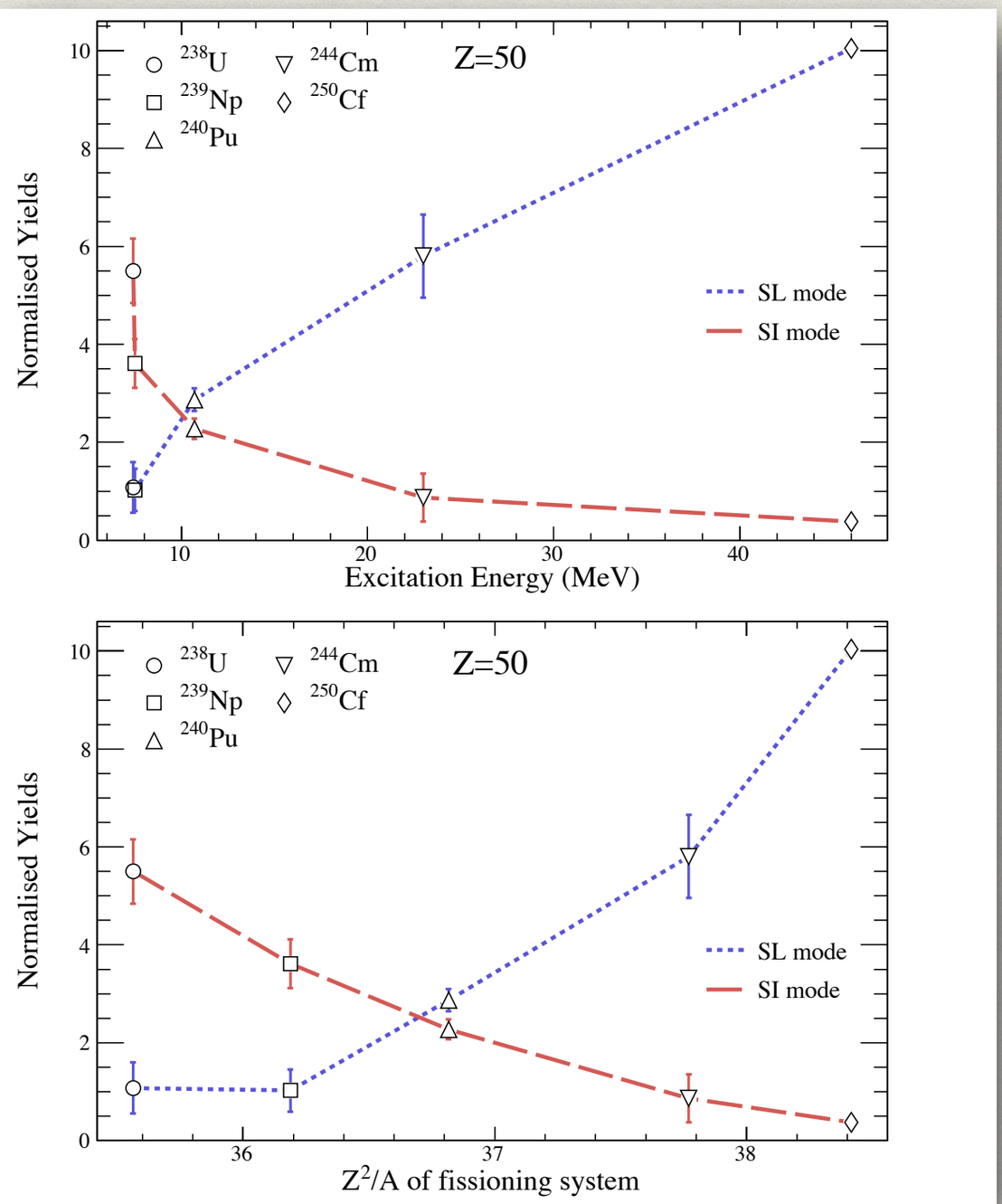

- The isotopic distribution of Z=50 is mainly described by two fission modes: SL, related to the symmetric fission and SI, related to spherical closed shells (N=82, Z=50)
- The **E_x feeds the SL mode** while the **SI mode shows an interplay between the E_x and the fissility parameter**

CONCLUSIONS

- The use of inverse kinematics with the VAMOS spectrometer allowed the characterization of fissioning system in terms of Z, A, and E_x, and the isotopic identification of their full fragment distribution.
- The measured elemental and neutron yield distributions show a dominant effect of structure at low E_x, while at higher E_x, the macroscopic features become more relevant. Maxima of production are observed in Z=40 and N=60,82.
- The local even-odd effect is found to increase around Z~50 splits, consistent with a larger binding energy, and at high asymmetry.
- The correlation between N and Z also reveals the effect of structure: a charge polarization with a saw-tooth behavior appears with a maximum governed by ^{132}Sn. Again, increasing E_x reduces this structure effect, but mainly on the heavy fragment.
- The isotopic distributions of Z=50 suggest that the SL mode is mainly governed by E_x while the SI shows also the impact of the fissility.

MASS FISSION YIELDS

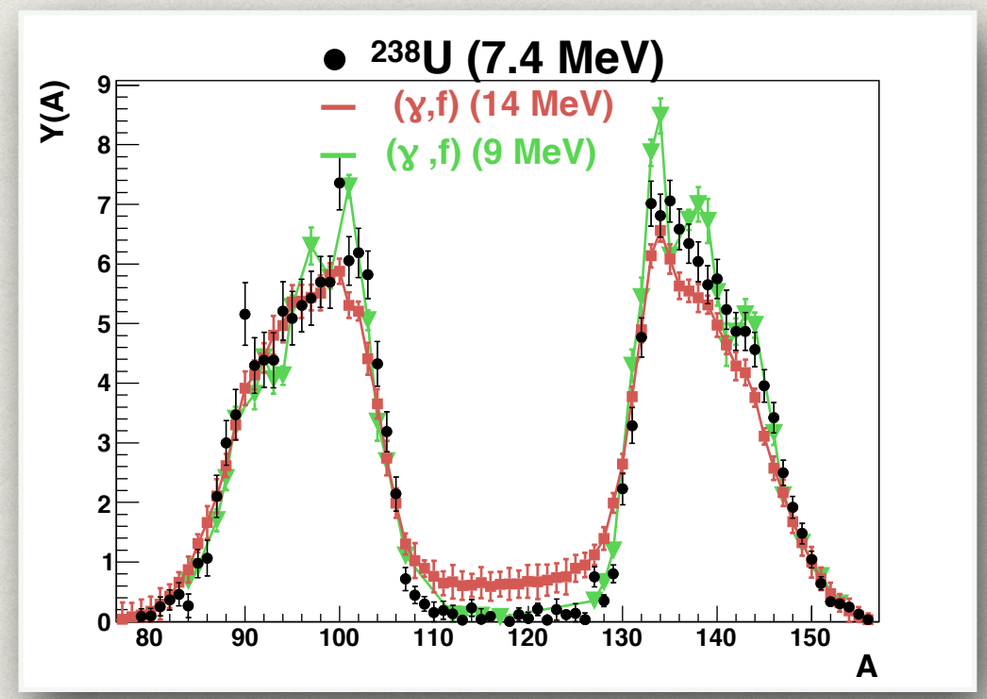

E. Pelleareau et al. PRC 95 (2017) 054603
H. Naik et al. EPJA 49 (2013) 94

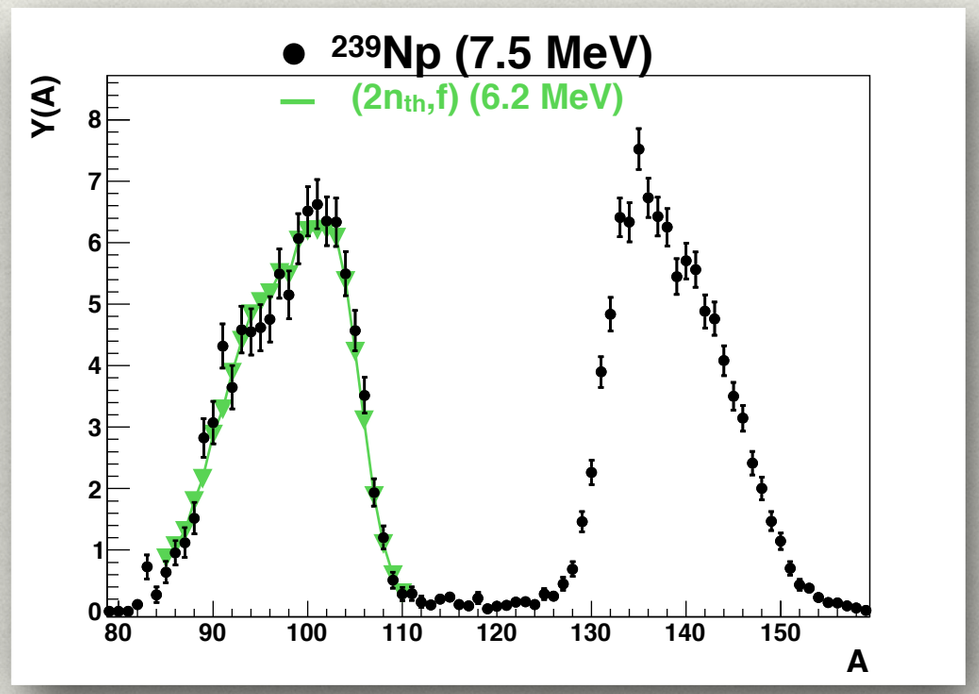

G. Martinez et al. NPA 515 (1990) 433

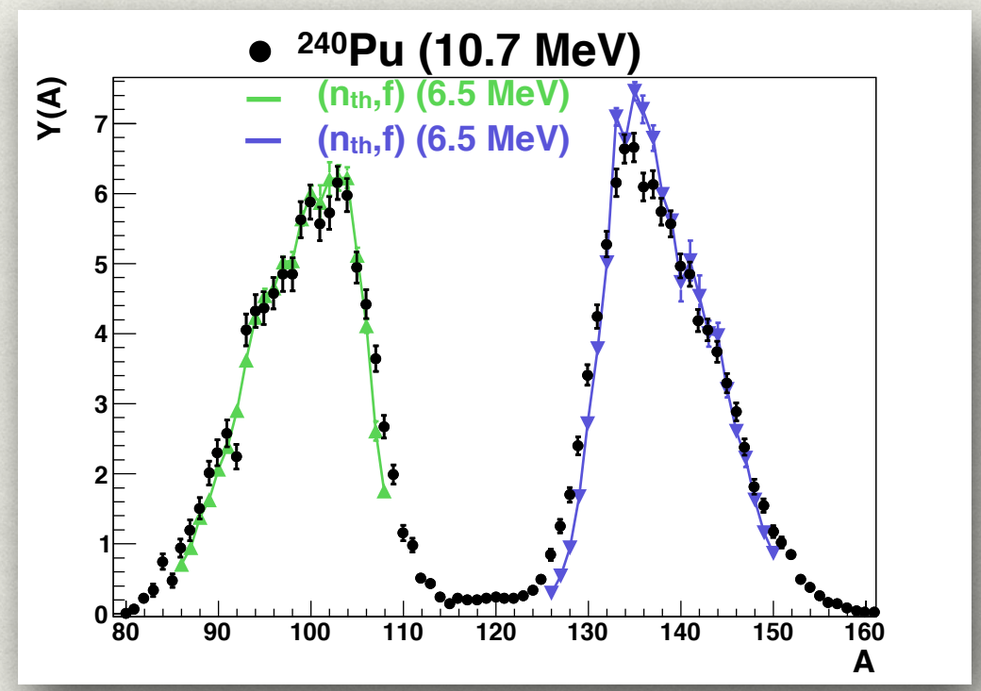

C. Schmitt et al. NPA 430 (1984) 21
A. Bail et al. PRC 84 (2011) 034605

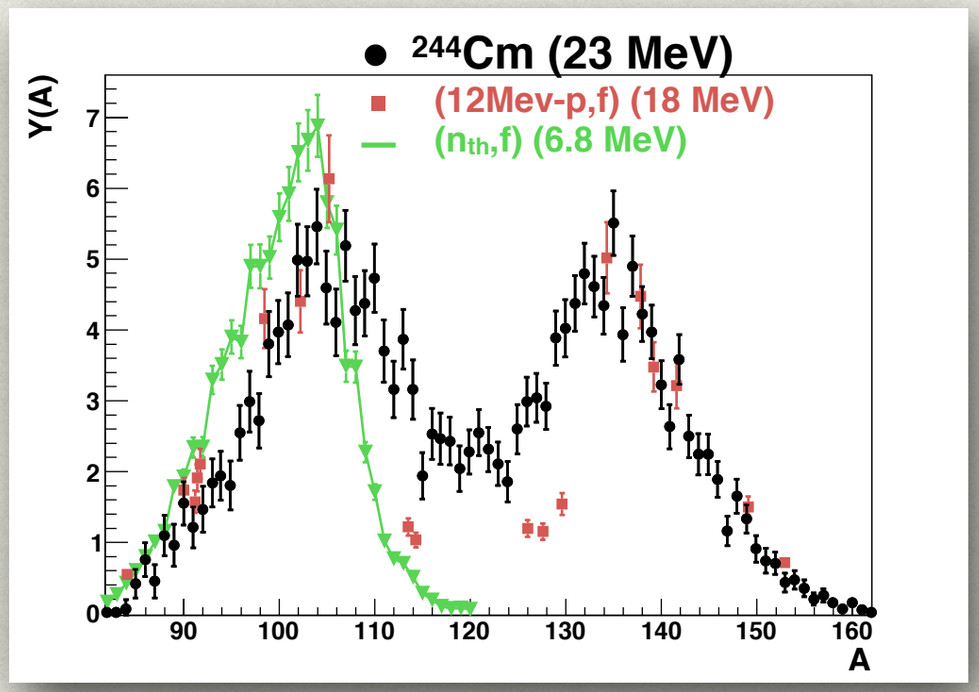

T. Ohtsuki et al. PRC 40 (1989) 2144
I. Tsekhanovich et al. PRC 70 (2004) 044610

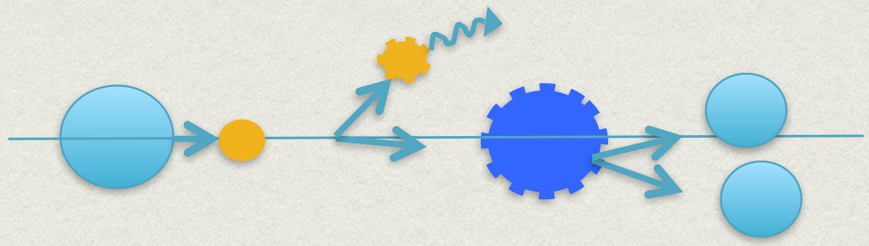

EXOGAM detector allow us to evaluate the excitation probability of the target-like nuclei

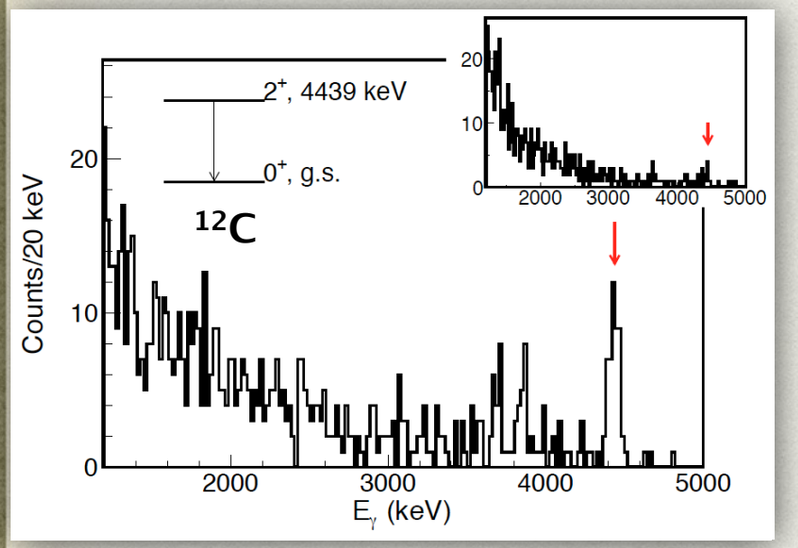

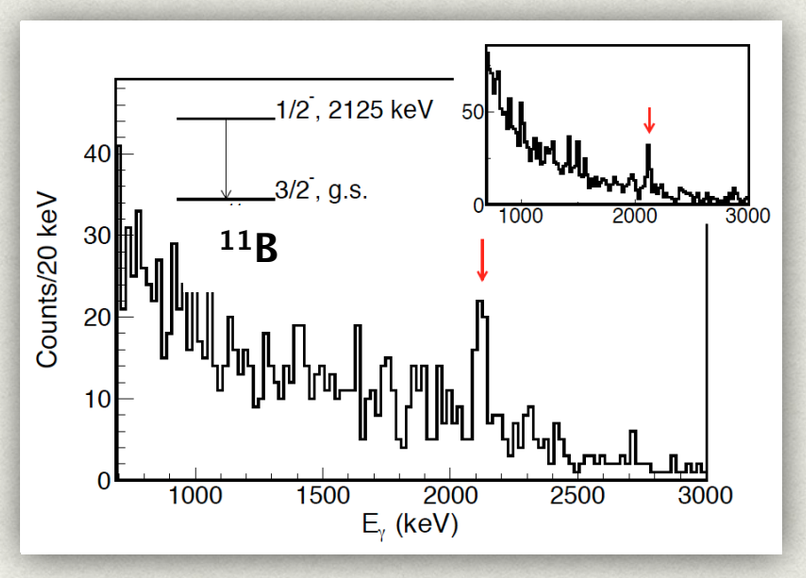

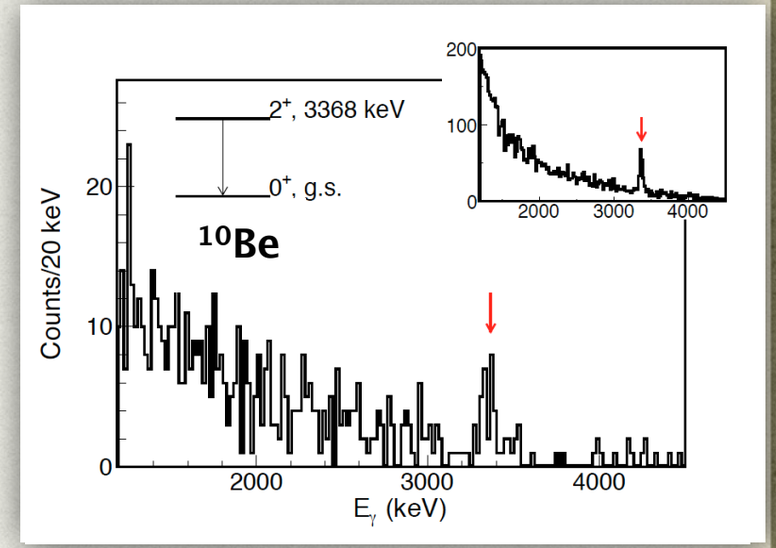

γ-rays measurements show excited states in ^{12}C, ^{11}B and ^{10}Be **in coincidence with fission with P_γ = 0.12-0.14**

C. Rodriguez-Tajes et *al.*,
PRC 89 (2014) 024614

Wilkins Scission Point

$$R = R_0(1 + \frac{2}{3}\beta)$$

$$r = R_0(1 - \frac{1}{3}\beta)$$

$$V = V_1^{LDM} + V_2^{LDM} + S_1^N + S_2^N + S_1^Z + S_2^Z + P_1^N + P_2^N + P_1^Z + P_2^Z + V_{12}^{Coulomb} + V_{12}^{Nuclear}$$

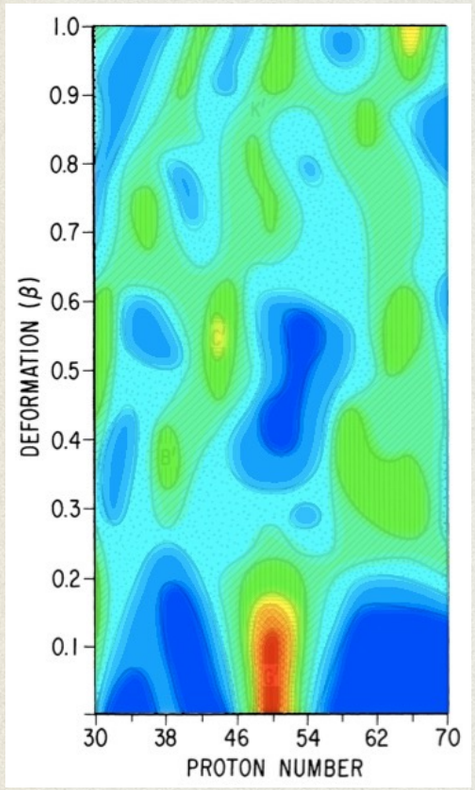

Brosa Random neck rupture

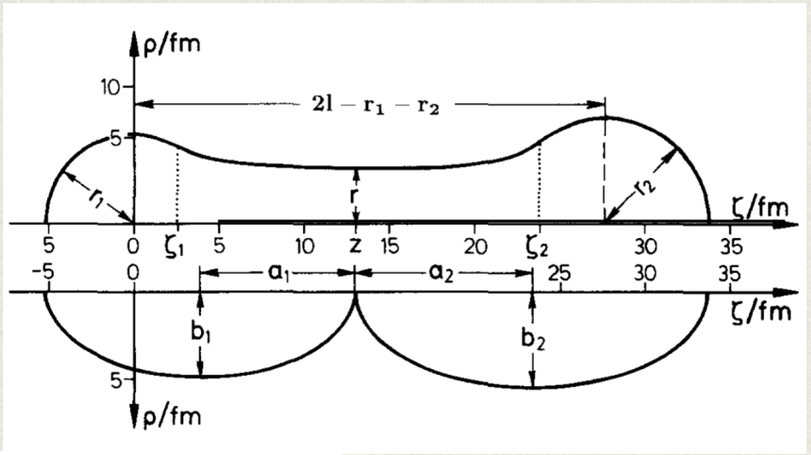

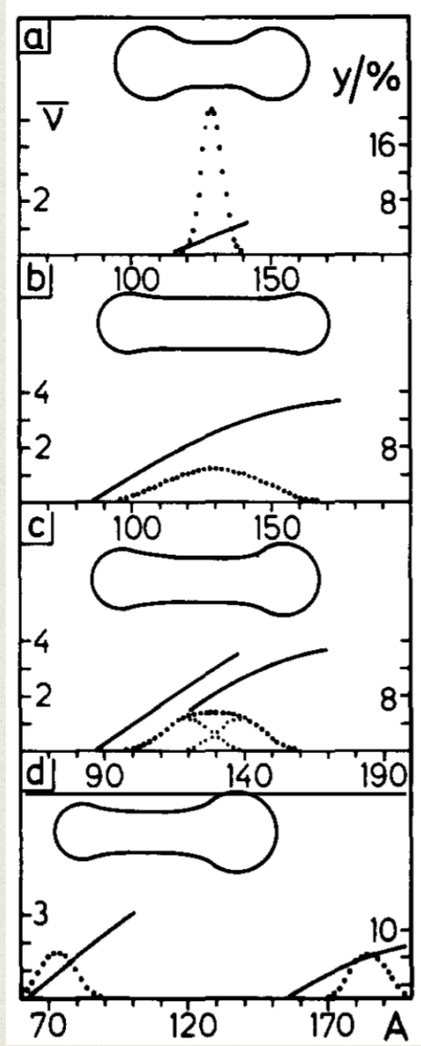

Super short channel

Super long channel

Standard I channel

Super asymmetric channel

GEF calculation

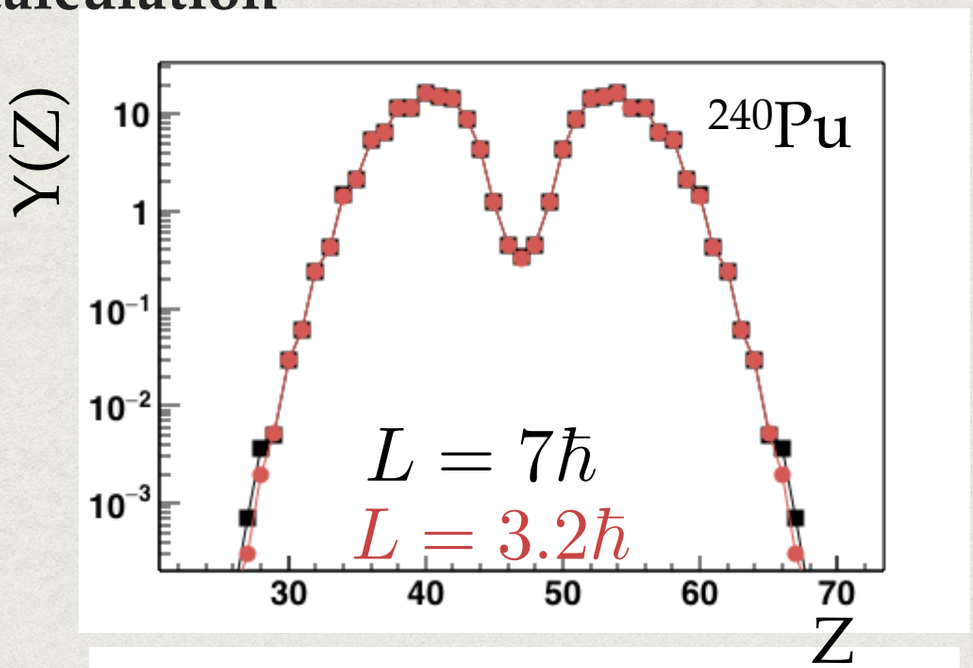

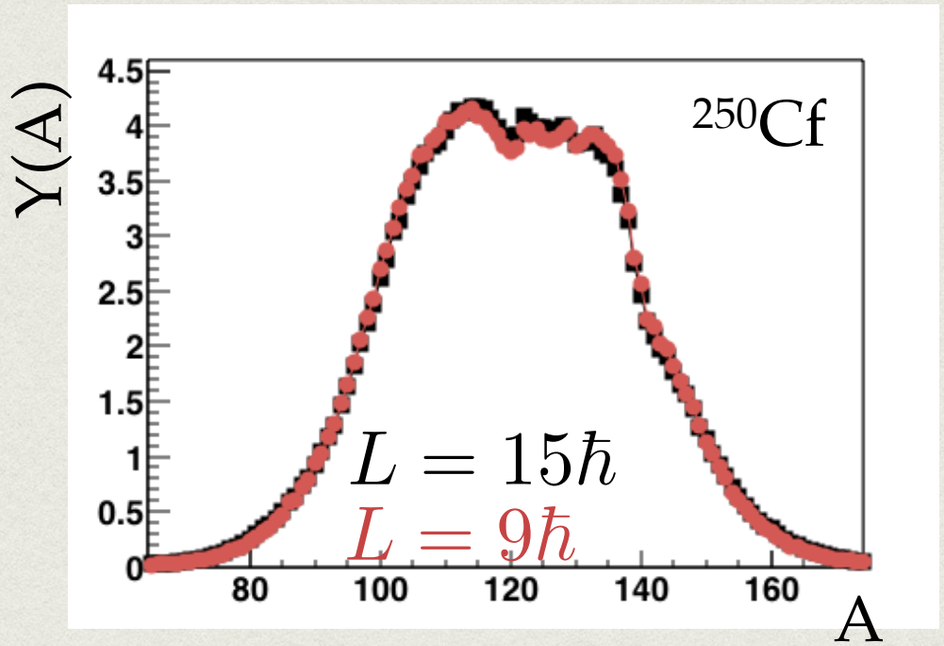

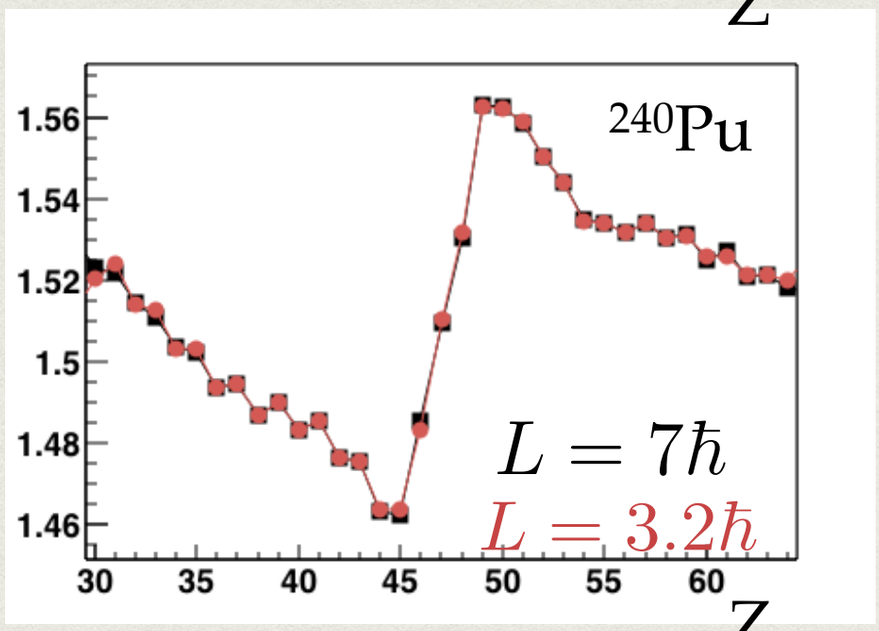

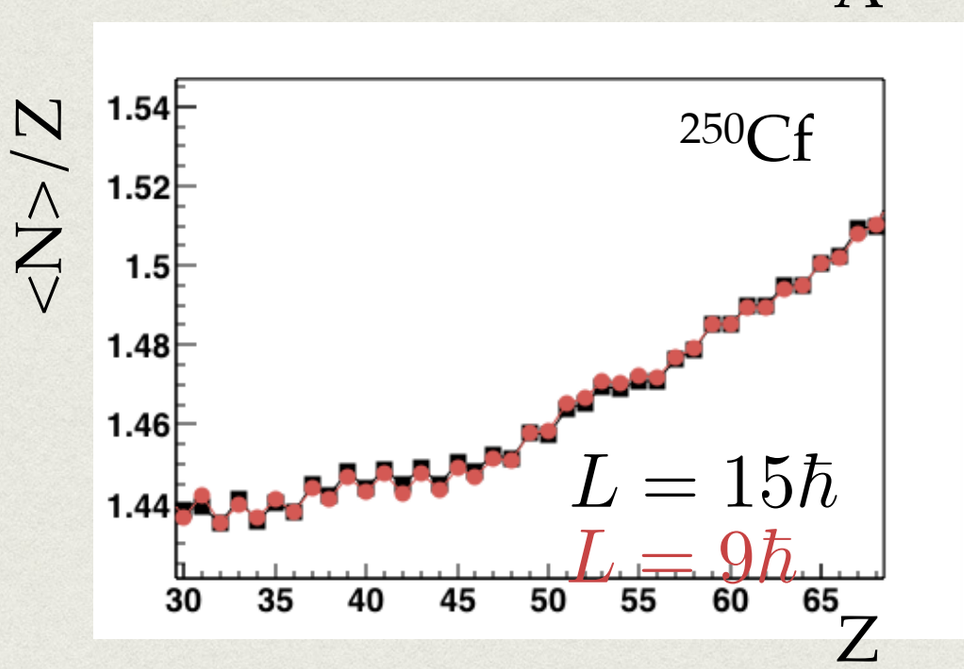

$\langle\nu\rangle = 3.47$ $\langle\nu\rangle = 3.46$

$\langle\delta\rangle = 9.51$ $\langle\delta\rangle = 9.66$

$\langle\nu\rangle = 8.79$ $\langle\nu\rangle = 8.79$

$\langle\delta\rangle = 3.91$ $\langle\delta\rangle = 3.99$

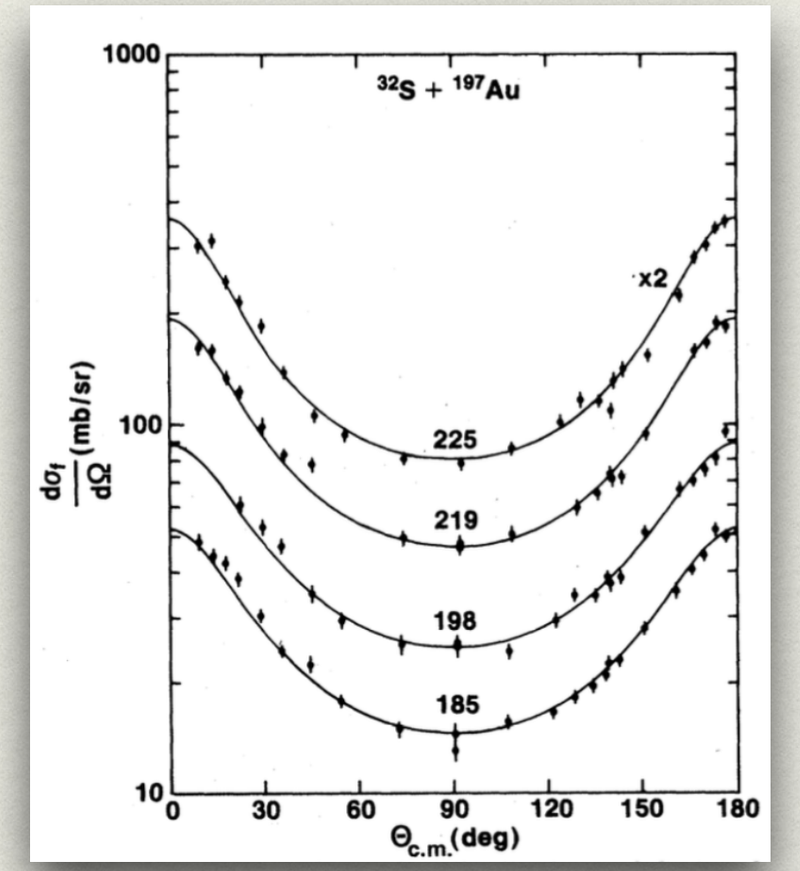

B. B. Back et al. PRC 32 (1985) 195

$$W(\theta_{CM}) = W(90^\circ)\left[1 + \alpha\cos^2(\theta_{CM})\right]$$

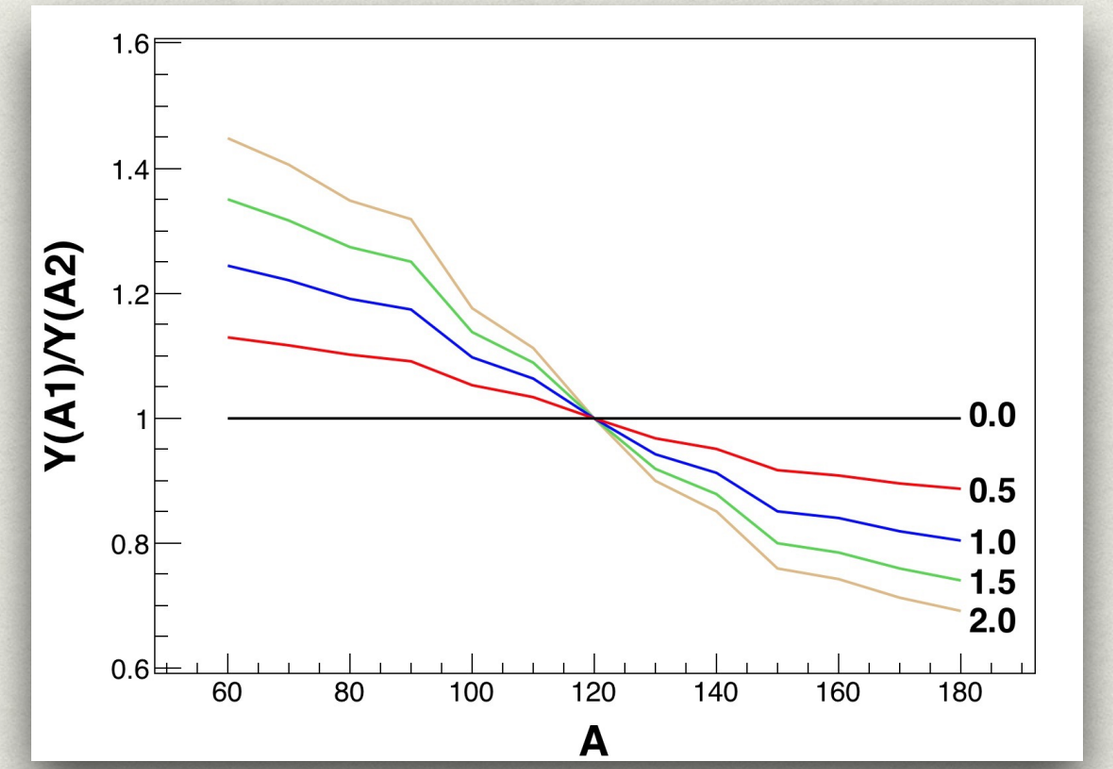

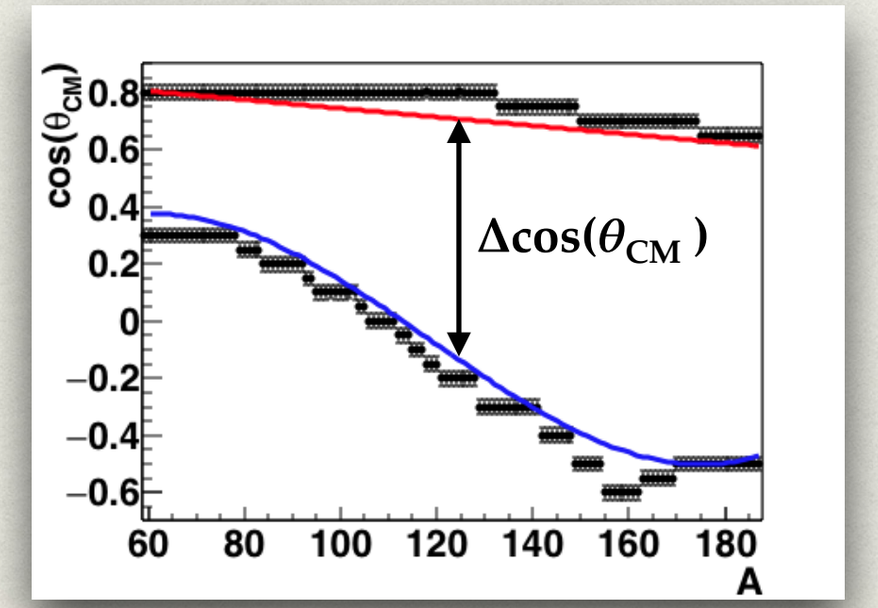

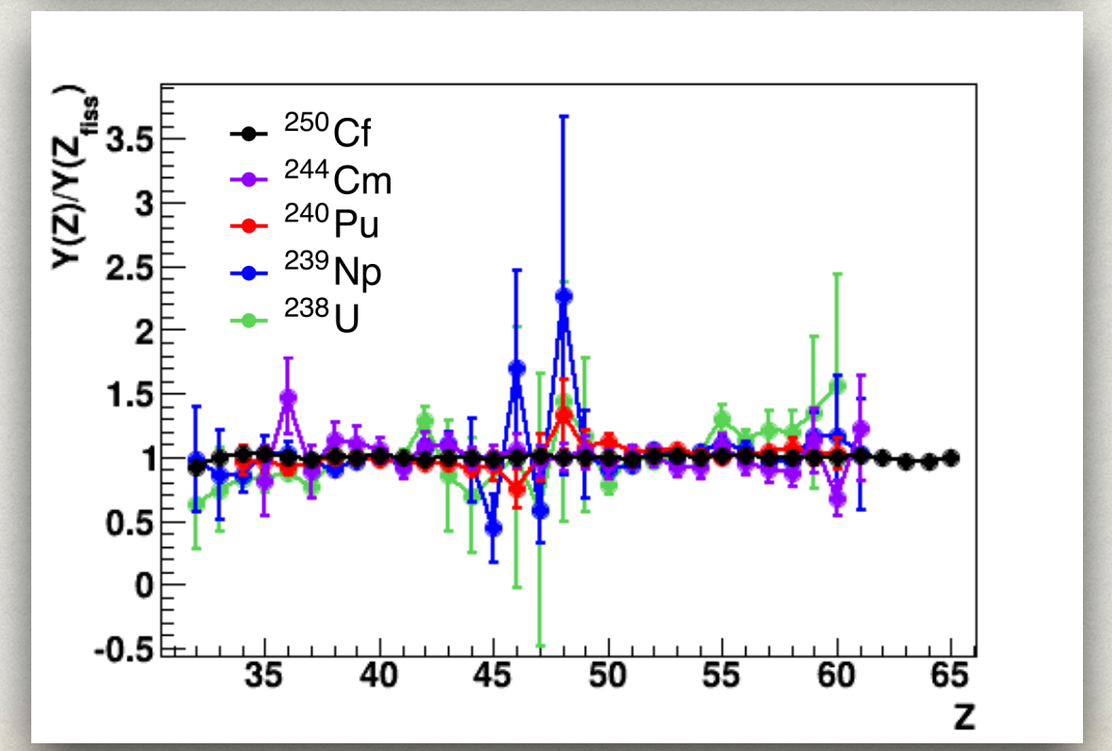

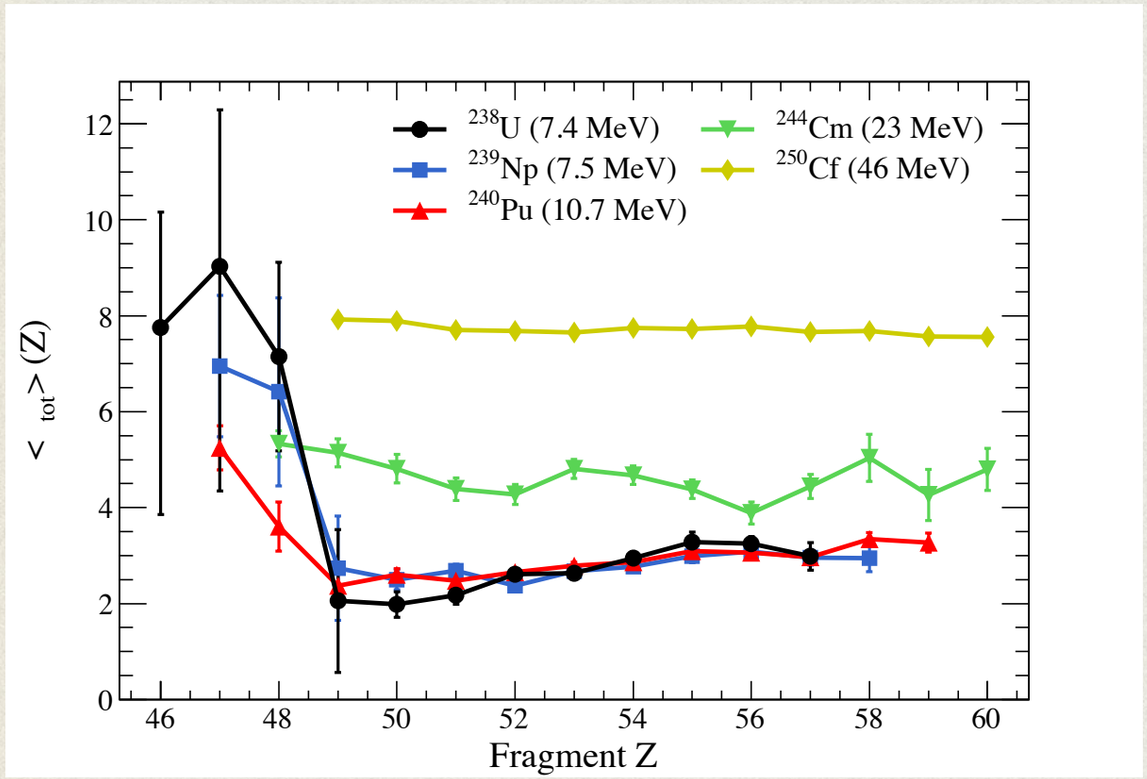
^{238}U (7.4 MeV)
^{239}Np (7.5 MeV)
^{240}Pu (10.7 MeV)
^{244}Cm (23 MeV)
^{250}Cf (46 MeV)
< $_{tot}$> (Z)
Fragment Z

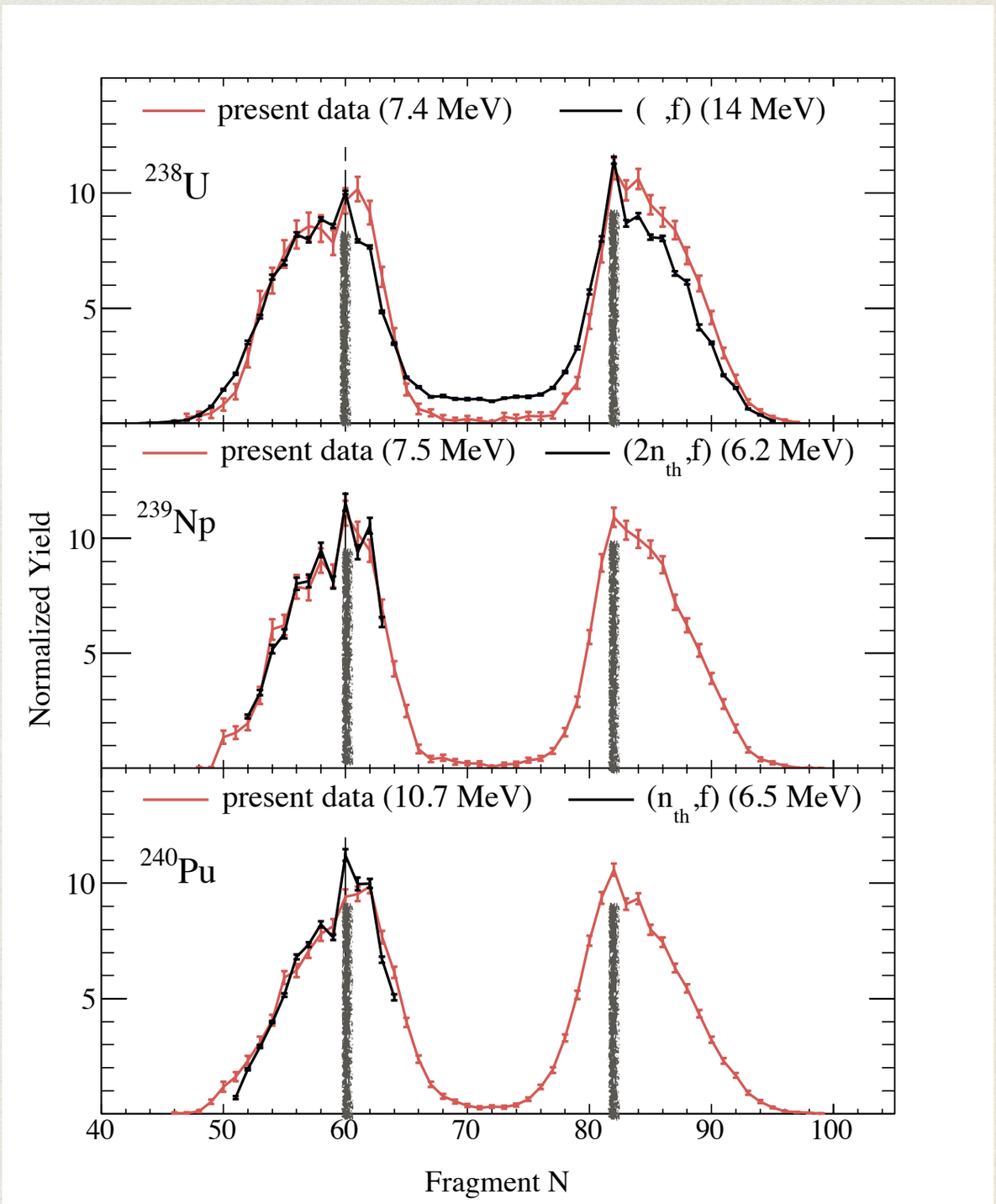
present data (7.4 MeV)
(,f) (14 MeV)
^{238}U
present data (7.5 MeV)
(2n$_{th}$,f) (6.2 MeV)
^{239}Np
present data (10.7 MeV)
(n$_{th}$,f) (6.5 MeV)
^{240}Pu
Normalized Yield
Fragment N

^{238}U

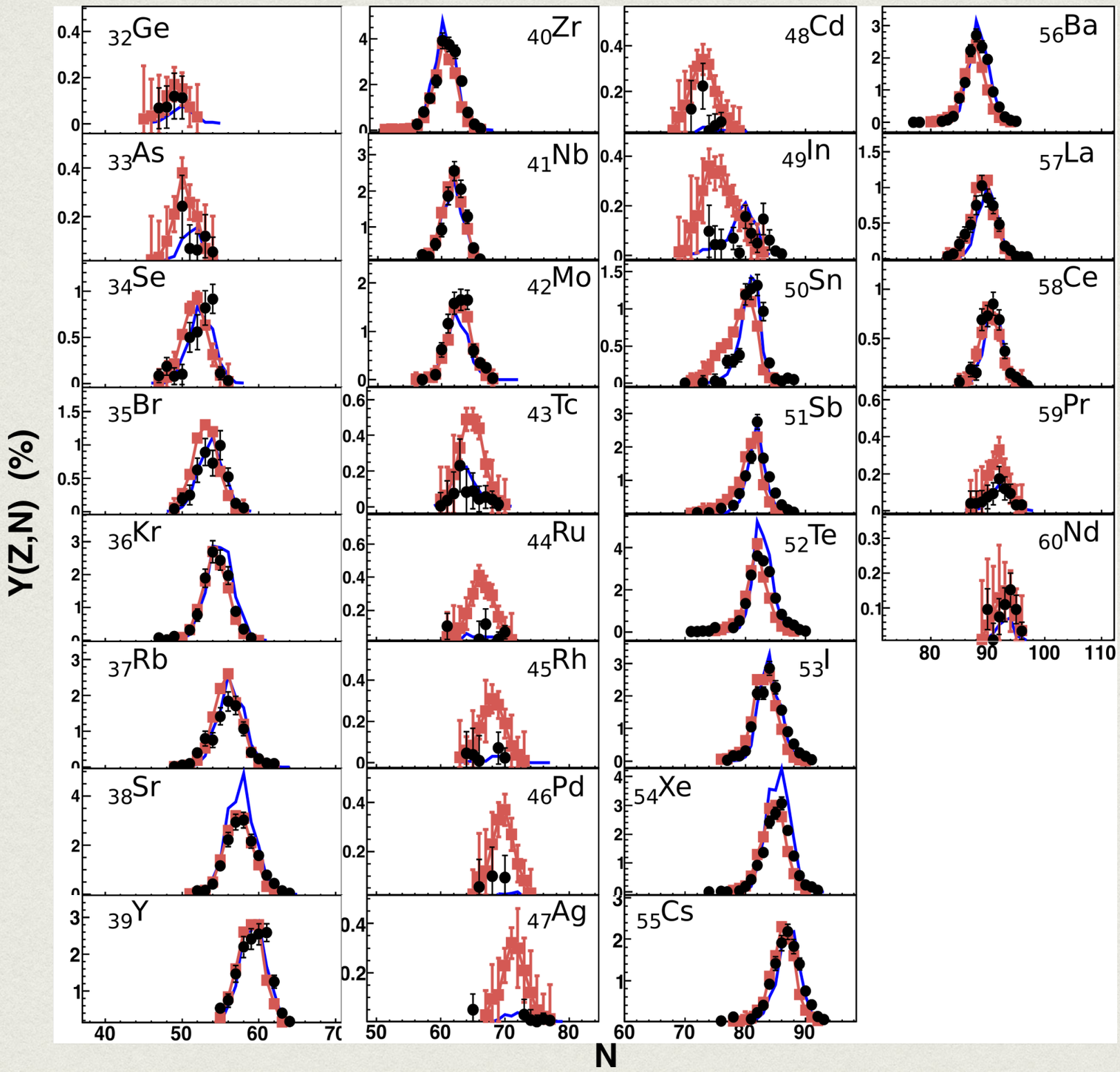
Y(Z,N) (%)
N
32Ge
33As
34Se
35Br
36Kr
37Rb
38Sr
39Y
40Zr
41Nb
42Mo
43Tc
44Ru
45Rh
46Pd
47Ag
48Cd
49In
50Sn
51Sb
52Te
53I
54Xe
55Cs
56Ba
57La
58Ce
59Pr
60Nd

^{239}Np

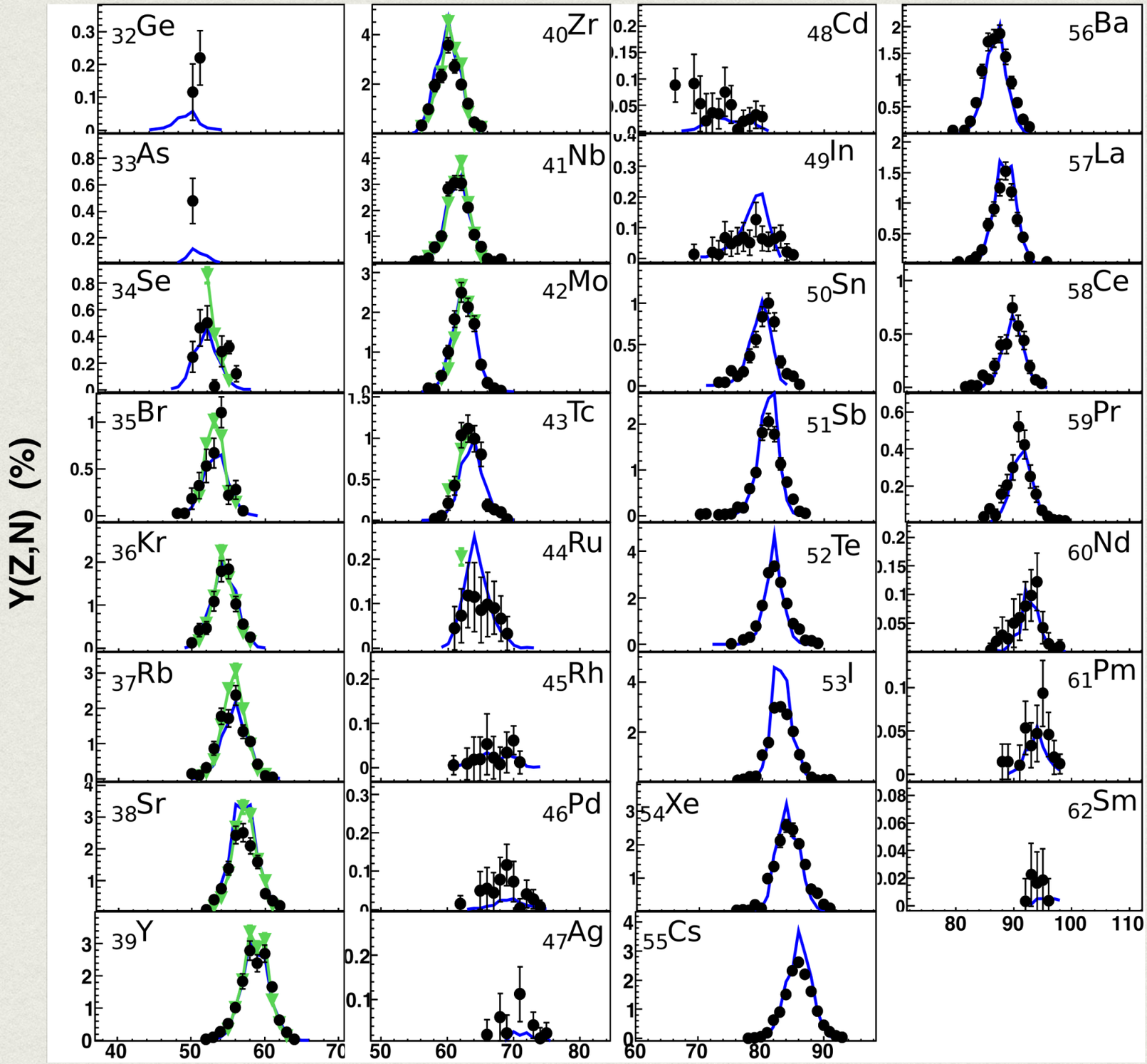
Y(Z,N) (%)
N
32Ge
33As
34Se
35Br
36Kr
37Rb
38Sr
39Y
40Zr
41Nb
42Mo
43Tc
44Ru
45Rh
46Pd
47Ag
48Cd
49In
50Sn
51Sb
52Te
53I
54Xe
55Cs
56Ba
57La
58Ce
59Pr
60Nd
61Pm
62Sm

^{240}Pu

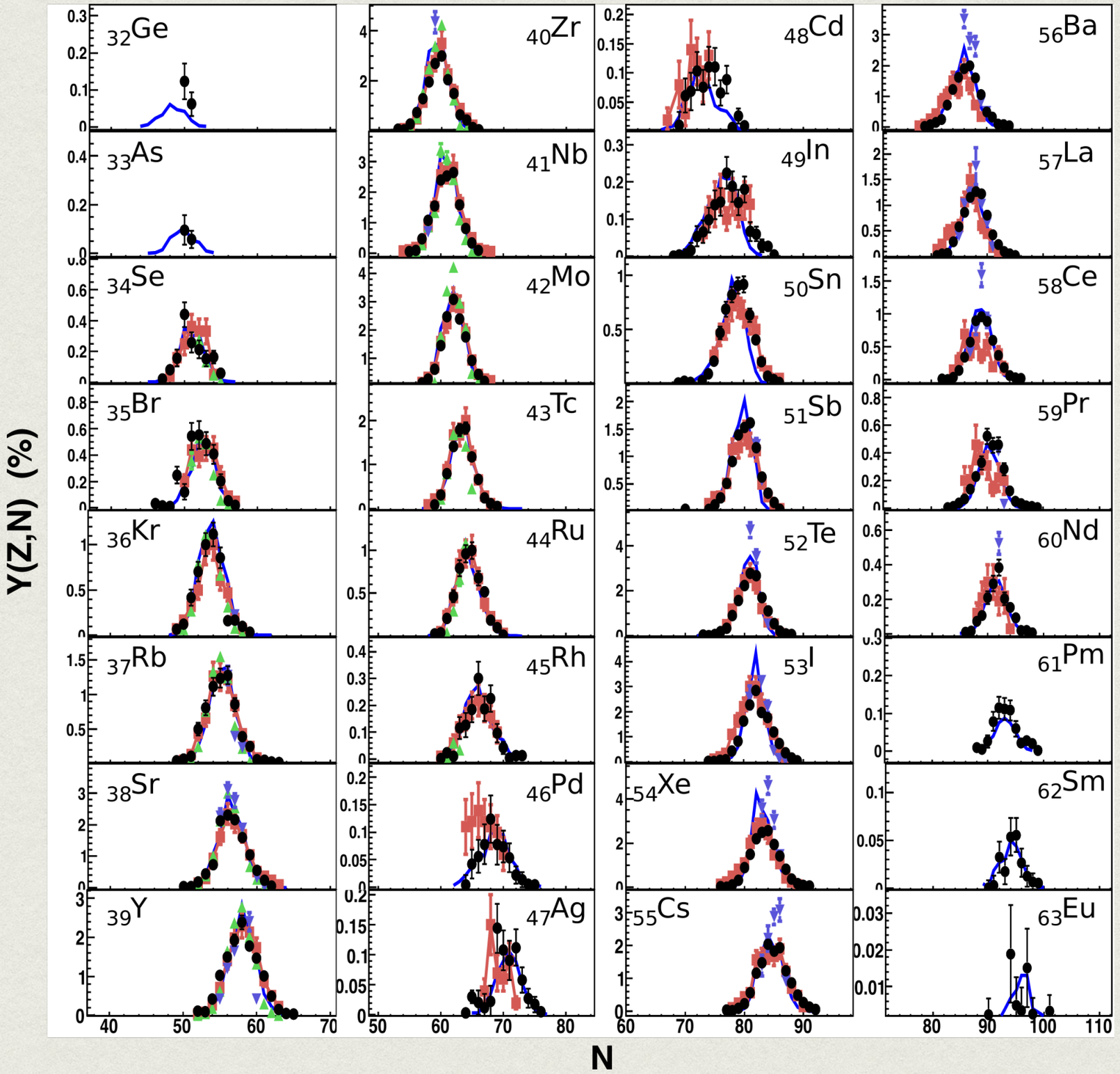
Y(Z,N) (%)
N
32Ge
33As
34Se
35Br
36Kr
37Rb
38Sr
39Y
40Zr
41Nb
42Mo
43Tc
44Ru
45Rh
46Pd
47Ag
48Cd
49In
50Sn
51Sb
52Te
53I
54Xe
55Cs
56Ba
57La
58Ce
59Pr
60Nd
61Pm
62Sm
63Eu

^{244}Cm

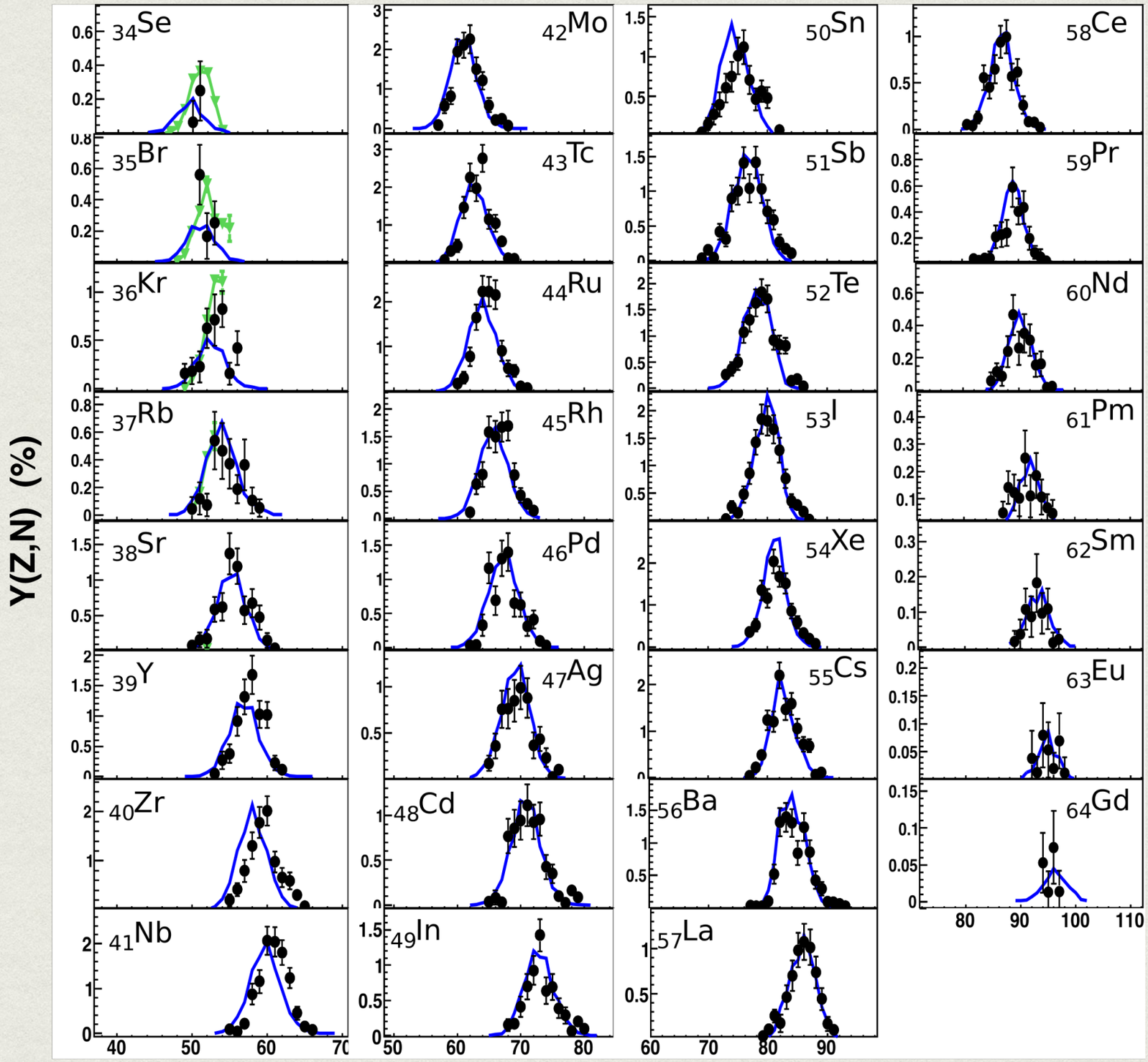
Y(Z,N) (%)
N
34Se
35Br
36Kr
37Rb
38Sr
39Y
40Zr
41Nb
42Mo
43Tc
44Ru
45Rh
46Pd
47Ag
48Cd
49In
50Sn
51Sb
52Te
53I
54Xe
55Cs
56Ba
57La
58Ce
59Pr
60Nd
61Pm
62Sm
63Eu
64Gd

^{250}Cf

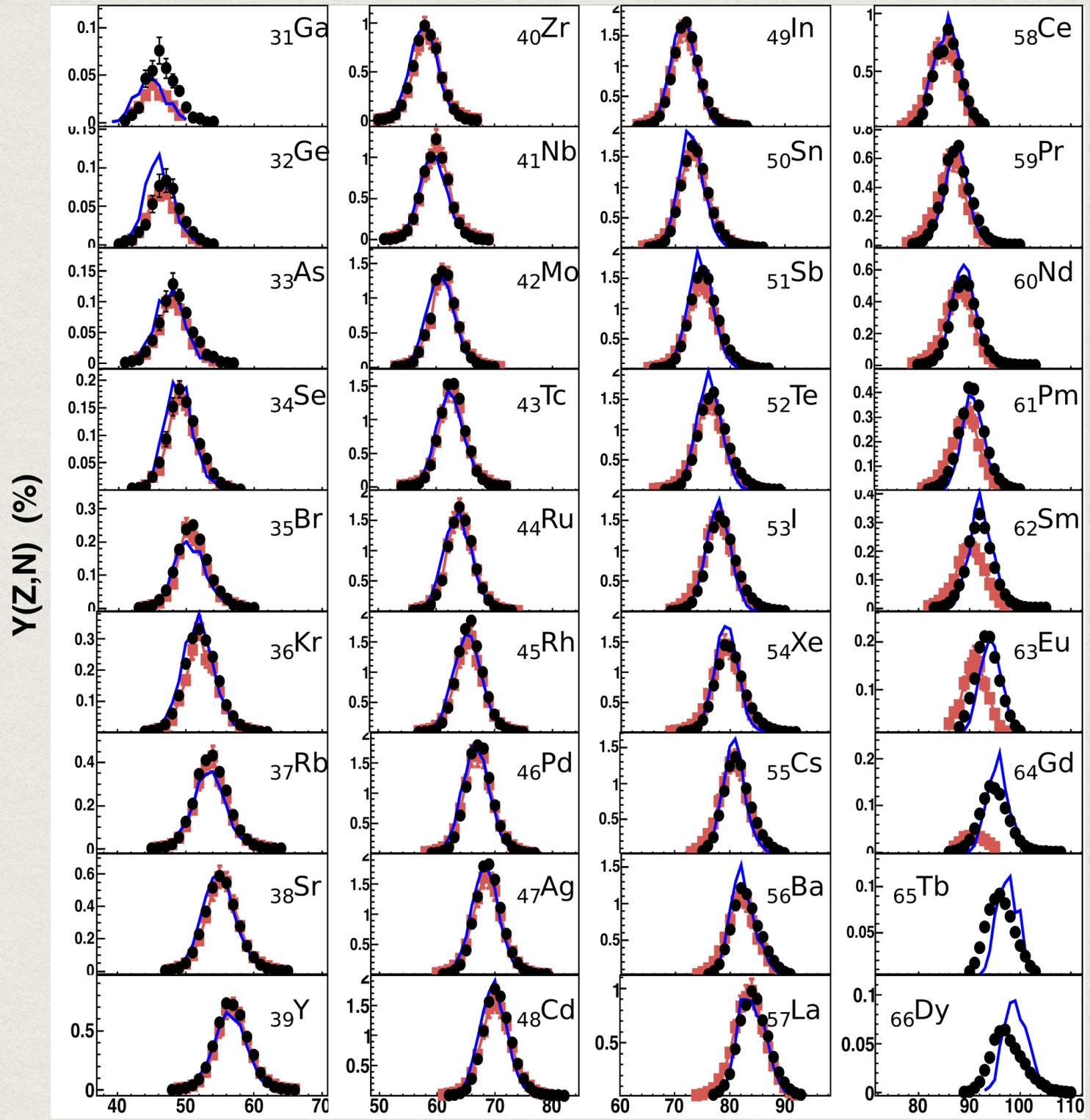
Y(Z,N) (%)
N
31Ga
32Ge
33As
34Se
35Br
36Kr
37Rb
38Sr
39Y
40Zr
41Nb
42Mo
43Tc
44Ru
45Rh
46Pd
47Ag
48Cd
49In
50Sn
51Sb
52Te
53I
54Xe
55Cs
56Ba
57La
58Ce
59Pr
60Nd
61Pm
62Sm
63Eu
64Gd
65Tb
66Dy